Final version published as: Overton JA, Cooke DF, Goldring AB, Lucero S, Weatherford C, Recanzone GH. (2017) Improved methods for acrylic-free implants in non-human primates for neuroscience research. *Journal of Neurophysiology*, 118, 3252–3270. doi:10.1152/jn.00191.2017

TITLE PAGE

Title:

Improved methods for acrylic-free implants in non-human primates for neuroscience research

Running Head: Improved methods for acrylic-free implants in NHP

Authors and author addresses:

Jacqueline A. Overton[1], Dylan F. Cooke[2], Adam B. Goldring[1], Steven A. Lucero[3], Conor Weatherford[1], Gregg H. Recanzone[1,4]

[1]Center for Neuroscience, Univ. of California, Davis, CA 95616, USA

[2]Dept. of Biomedical Physiology and Kinesiology, Simon Fraser University, Burnaby, British Columbia, Canada

[3]Dept. of Biomedical Engineering, Physiology and Behavior, Univ. of California, Davis, CA 95616, USA

[4]Department of Neurobiology, Physiology and Behavior, Univ. of California, Davis, CA 95616, USA

Corresponding Author:

Jacqueline A. Overton

Center for Neuroscience,

1544 Newton Ct.,

Univ. of California, Davis, CA 95616, USA

jaoverton@ucdavis.edu

Figures: 8

Keywords: monkey; implant; neurophysiology; osseointegration; biocompatibility

Conflict of interest: None

ABSTRACT

Traditionally, head fixation devices and recording cylinders have been implanted in non-human primates (NHP) using dental acrylic, in spite of several shortcomings associated with acrylic. The use of more biocompatible materials such as titanium and PEEK is becoming more prevalent in NHP research. We describe a cost-effective set of procedures that maximizes the integration of headposts and recording cylinders with the animal's tissues while reducing surgery time. Nine rhesus monkeys were implanted with titanium headposts and one of these was also implanted with a recording chamber. In each case, a 3D printed replica of the skull was created based on computerized tomography scans. The titanium feet of the headposts were shaped and the skull thickness measured pre-operatively, reducing surgery time by up to 70%. The recording cylinder was manufactured to conform tightly to the skull, which was fastened to the skull with 4 screws and remained watertight for 8.5 months. We quantified the amount of regression of the skin edge at the headpost. We found a large degree of variability in the timing and extent of skin regression that could not be explained by any single recorded factor. However, there was not a single case of bone exposure: while skin retracted from the titanium, skin also remained adhered to the skull adjacent to those regions. The headposts remained fully functional and free of complications for the experimental life of each animal, several of which are still participating in experiments over 4 years after implant.

NEW & NOTEWORTHY

Cranial implants are often necessary for performing neurophysiology research with nonhuman primates. We present methods for using 3D printed monkey skulls to form and fabricate acrylic-free implants pre-operatively in order to decrease surgery times and the risk of complications and increase the functional life of the implant. We focused on reducing costs, creating a feasible timeline, and ensuring compatibility with existing laboratory systems. We discuss the importance of using more biocompatible materials and enhancing osseointegration.

INTRODUCTION

Nonhuman primates (NHP) are indispensable animal models of human biology and medicine and are used in a wide range of fields, including immunology, microbiology, and genetics. In neuroscience, research with NHP has furthered our understanding of normal neuronal functioning such as sensory processing (e.g., Goodale and Milner 1992; Parker and Newsome 1998; Sunkaraa et al., 2016), motor control (e.g., Mink 1996; Plautz et al. 2000; Graziano et al. 2002; Hwang et al., 2013), learning and memory (e.g., Squire and Zola-Morgan 1991; Miller and Cohen 2001; Konecky et al., 2017), and attention (e.g., Desimone and Duncan 1995; Luck et al. 1997; Verhoefl and Maunsell, 2017). Similarly, NHP research

has provided invaluable insights into neurological disorders such as Parkinson's disease (e.g., Fearnley and Lees 1991; Bergman and Deuschl 2002; Potts et al., 2014), cognitive impairment (e.g., Burke and Barnes 2006; Morrison and Baxter 2012), and stroke (e.g., Nudo and Milliken 1996; Nudo et al. 1996; Fan et al., 2017). A valuable technique in neuroscience research involves recording or manipulating neuronal activity in NHP while they are alert and performing a behavioral or perceptual task. Such studies were initiated about 50 years ago (e.g., Wurtz 1968), and continue to this day in a variety of both cortical and sub-cortical brain areas. This research relies on chronic cranial implants. One implant, the headpost (see Figure 1), allows the researcher to stabilize the animal's head during behavioral training and experimentation. A cranial implant may also consist of one or more recording chambers, which allows the researcher to gain access to the brain for recording data or other experimental manipulations such as microstimulation or local inactivation. Head fixation is essential for physiological recording and important for maintaining head position in many sensory experiments, particularly those involving the visual or auditory systems. Thus, headpost and recording chamber implants are an integral part of many avenues of neuroscience research in NHP.

Polymethyl methacrylate (PMMA, alternatively called "acrylic", "dental acrylic" or "bone cement") is the most popular method of affixing cranial implants to the skull, primarily due to the ease with which it can be modelled *in situ* to form a customized fit (see Adams et al., 2011). In this technique, the skull is exposed and screws are placed in the skull around the position of the implanted headpost and/or recording cylinder(s). The implant hardware is held in place with a stereotaxic manipulator while the PMMA is mixed and poured onto the exposed skull to cover the screws and part of the implant hardware. Once cured, the PMMA mass secures the implant hardware, anchored to the skull via the bone screws. This technique has been used extensively, primarily because it is low cost, and can be customized to individual NHPs depending on the location of the headpost and the number of recording cylinders. Additionally, it is radio transparent, and with non-ferrous screws and other components of the implant can allow for subsequent MRI imaging to verify cylinder placement, etc. Finally, in some instances pre-surgical imaging may not be possible, or novel hardware may need to be incorporated into an existing implant, in which case the acrylic method allows for some flexibility during surgery.

Nonetheless, this technique presents several common problems. The acrylic that supports the headpost (see Figure 1A) can be gradually weakened with time and use and is prone to breakage, potentially leading to exposure of the underlying bone. Also, an infection underneath the acrylic implant can lead to a dramatic thinning of the underlying bone and enlargement of the screw holes and craniotomy sites (see Fig. 1 in Adams et al. 2011), and may lead to implant failure. Implant breakages and infections require

repair or removal and replacement of the implant, which puts the animal at increased risk due to additional procedures and halts the progress of research.

Creating the implant during surgery is time-consuming and requires considerable expertise to do properly. The NHP acrylic implant is formed intraoperatively by mixing PMMA powder with liquid methyl methacrylate (MMA); the mixture is then poured over the exposed skull. One challenge is that the acrylic must be poured smoothly without introducing bubbles or fissures, and yet prevented from leaking to tissue outside of the intended implant boundary or into craniotomies where the recording chambers are being positioned. It is thought that crevices introduced into the acrylic when it is poured may harbor bacteria and lead to infection. The viscosity of the PMMA/MMA mixture when it is poured can be controlled by the surgeon depending on the time elapsed from the initial mixture. The polymerization reaction during the curing process is exothermic, reaching temperatures up to 110°C, which can lead to necrosis of surrounding tissue (Leggat et al. 2009) if not cooled continuously with saline (Genest 1978). Although different additives, such as castor oil (Lopez et al., 2011; Tai et al., 2016) or pre-cooling (Lai et al., 2012; Tai et al., 2016) can reduce this maximum temperature to around 60°C, this is still hot enough to cause necrosis (Gergely et al., 2016). To allow the NHP implant to cool sufficiently, it must be built very gradually with several small batches of acrylic. The process of building up and cooling the acrylic often accounts for >50% of the duration of the surgery. Therefore, there is a need for an implant technique that is technically less challenging for the researcher to perform, decreases surgery times and reduces the risk of complications such as infection and heat damage.

Use of PMMA is valuable in the operating room with human patients, but use in humans raises a number of concerns as well. PMMA is the most commonly used material for cranioplasty (repairing craniectomies or cranial defects) in humans because it is sufficiently durable, radiologically transparent and easy to mold and modify while being relatively inexpensive (Lee et al. 2009; Aydin et al. 2011; Caro-Osorio et al. 2013). Human cranioplasty is sometimes performed in a manner similar to the NHP implant, where the PMMA/MMA mixture is poured over the dura mater during surgery. Caro-Osorio et al. (2013) reported overall PMMA-cranioplasty-associated complications in human patients to be between 9.2 - 23%, with infection being the main concern, reported in 9.2 - 19% of cases. Pre-molding PMMA implants has been found to significantly decrease rates of infection (Lee et al. 2009; Caro-Osorio et al., 2013) as well as operation times (40 mins faster; Lee et al. 2009). Unfortunately, prefabrication of an acrylic implant for NHP research would void the primary advantage for using acrylic, which is the ability to pour and form *in situ* and thus achieve a perfect fit. However, pre-fabricating implants is a practicable way to decrease surgery times which is known to decrease the risk of surgical site infections (Mangram et al. 1999; APIC 2010).

An important difference between the human cranioplasty and NHP acrylic implant techniques is how they impact surrounding soft tissues, particularly the skin. Whereas the cranioplasty is covered with muscle and skin and resides entirely within the body, the percutaneous primate implant introduces an implant margin (Fig. 1A) that is an avenue to infection and must be cleaned and maintained frequently. Also, residual chemicals in the PMMA matrix may be toxic, for example the monomer form of acrylic, MMA, is known to be a skin and respiratory irritant and is cytotoxic in many cases, including to endothelial cells (Leggat et al. 2009) which may lead to irritation at the implant margin. A related factor with respect to the skin in NHP acrylic implants is granulation tissue, a highly vascular connective tissue that is a normal part of wound healing but obstructive to a healthy percutaneous implant margin. It proliferates along the implant margin and in some cases, grows between the acrylic implant and the bone, weakening the implant. Therefore, an implant technique that preserves the integrity of soft tissue and decreases maintenance and implant margin complications would be a marked improvement. While PMMA is a versatile material that is still used in humans, there are a variety of newer, more biocompatible materials being used in cranioplasty and a variety of other human implants that overcome some of the limitations discussed above.

Choosing an implant material depends on the properties of the material (e.g., strength, durability and biocompatibility) as well as on the specific application and stresses that will be exerted on the implant. For example, dental implants must withstand years of repetitive use and forces such as from chewing (Mandracci et al. 2016). Because of titanium's good biocompatibility, strength and ability to form a tight bond with bone tissue, or osseointegrate (Albrektsson et al. 1981; Tjellström et al. 1981), it is the material of choice for implant dentistry. Osseointegration is the preferred method of fixation for load-bearing implants in orthopedics and orthodontics (Hacking et al. 2012). For these reasons, titanium is an excellent material for use in NHP headpost implants.

When using an acrylic-free titanium implant it is important to consider factors that can encourage or impede osseointegration. Titanium integrates best with bone when it is tightly apposed to the bone surface, therefore it is critical to achieve as close a fit as possible (<1 mm) and maximize contact between bone and metal surfaces (Plecko et al. 2012). Modifying surface characteristics, such as roughening the implant surface can also improve osseointegration (Buser et al. 1991; Hacking et al. 2012). Application of hydroxyapatite (HA) as a paste during surgery (e.g., Adams et al. 2011) or as a coating applied to the titanium implant prior to surgery (Hacking et al. 2012; Mandracci et al. 2016) can further aid osseointegration.

Another highly biocompatible material, polyetheretherketone (PEEK), is a thermoplastic that is gaining in popularity for uses such as vertebra and hip replacements. PEEK has mechanical properties similar to bone and is not toxic to surrounding tissues. Unfortunately, PEEK does not integrate well with bone (Khoury et al. 2013; Ma and Tang 2014) and therefore is not ideal for load-bearing applications such as a headpost. However, PEEK has the advantage of being radiologically transparent, and therefore is preferred in applications where imaging of nearby tissues is required. This makes it a suitable material for non-load-bearing implants such as the recording chamber (Fig. 1). Whereas the recording chamber is traditionally embedded in the acrylic implant (Fig. 1A), recent studies have used an acrylic-free PEEK recording chamber for NHP neuroscience research (McAndrew et al. 2012; Lanz et al. 2013).

ADOPTION OF ACRYLIC-FREE ALTERNATIVES

The use of acrylic-free implants using more biocompatible materials in NHP neurophysiology research is gaining popularity. Several attempts have been made to avoid the use of acrylic-embedded head-fixation devices in NHP research (Isoda et al. 2005; Adams et al. 2007; Davis et al. 2009; Lanz et al. 2013) or to eliminate the need for an invasively implanted cranially anchored fixation device entirely (Amemori et al. 2015; Drucker et al. 2015). Adams and colleagues developed a custom titanium footed headpost (2007) and recording chamber (2011) which were successfully implanted in several animals. McAndrew and colleagues (2012) designed a custom-fitted PEEK recording chamber that was screwed directly to the skull with titanium screws. Lanz and colleagues (2013) used Adams' headpost design, and designed a customized PEEK recording chamber using 3D printed skulls to aid in surgical planning. Acrylic-free titanium and PEEK implants are used exclusively at the Max Plank Institute for Biological Cybernetics (http://hirnforschung.kyb.mpg.de/en/methods/implant-technology.html). Despite these successes, the adoption of this new technique across other primate laboratories is slow. Given that cost and time constraints are potential factors to adoption, we focused on cost reduction and streamlining the timeline for implanting an acrylic-free titanium headpost and PEEK recording chamber.

Our goal was to devise a method for implanting monkeys with an acrylic-free implant while shortening surgery times, minimizing costs, and focusing on the ease of compatibility with existing systems. We drew on previous reports describing footed titanium headposts (Adams et al., 2007), a PEEK recording chamber (McAndrew et al. 2012) and the use of 3D printed skulls to guide surgical planning (Lanz et al. 2013). While our focus was on streamlining methods for an acrylic-free headpost, we also designed and implanted a custom-fitted PEEK recording chamber in one case. Special attention was paid to compatibility with existing systems, so we applied these methods with minor modifications in three

different laboratories that used slightly different hardware systems. We discuss these differences and compatibility issues where appropriate.

MATERIALS AND METHODS

Given our goal of reducing surgery times and the risk of complications, our methods focused on the pre-fabrication of implanted hardware using biocompatible materials. Briefly, we used a computed tomography (CT) scan of each animal's head to create a 3D printable digital model of the skull. The feet of the titanium headposts were bent prior to surgery to conform to a particular 3D printed skull replica. Magnetic resonance imaging (MRI) was also conducted and the CT and MRI data were co-registered to plan recording chamber locations. A recording chamber was designed using computer-aided design (CAD) software to mate perfectly with the skull in the desired location and 3D printed in PEEK. Our focus was on reducing costs without sacrificing quality or expediency and maintaining compatibility with existing experimental hardware. A summary and timeline of headpost-related procedures are provided in Table 1 and Figure 2, respectively. Here we describe how these methods were achieved.

SUBJECTS

We implanted 9 rhesus macaques (*Macaca mulatta*; 5 females, 4 males) with titanium footed headposts using the procedures that follow with slight variations between animals. Important differences between procedures used in cases are noted where appropriate. Rhesus macaques in this study ranged in age from 5.6 to 29.3 years at the time of implant surgery, corresponding to ~17 to ~88 human years (macaques age at approximately three times the rate of humans; Davis and Leathers 1985). Animals ranged in weight from 6 kg (female, case #5) to 13.5 kg (male, case #3), with most animals weighing 8 to 9 kg. Refer to Table 2 for information on each individual subject.

CT AND MRI SCANS

A CT scan of each animal's head was used to generate a digital model and physical replica of the skull to use for surgical planning and pre-fabrication of cranial implants. Note that the term "replica" will be used to refer to the physical 3D printed object, whereas "model" will be used when referring to the digital model or STL file. Scans were taken on a LightSpeed16 (General Electric) using 0.6 mm sequential slices. CT scans were obtained less than 6 months prior to planned surgeries. If more than 6 months had lapsed between an animals' CT scan and the implant surgery, the CT scans were repeated. In these cases, the second CT scan showed significant bone remodeling and changes to the skull surface topography, ultimately justifying the decision to repeat the scan. See Table 1 for timing of final CT scans relative to

surgeries and the duration that the animal had the headpost. In many cases we were able to complete the CT and have the digital model ready to print within one to two days (see Table 1 and Figure 2). In two cases, CT scans and surgeries were scheduled just two weeks apart, which was sufficient time to complete all steps. It should be noted that in many cases, the surgery date was delayed for reasons not related to implant readiness.

Structural MRIs were collected for 5 subjects in order to aid in localization of electrophysiology and stimulation targets within the brain. MRI scans were taken on a 3T Sigma Skyra scanner machine using T1 and T2 weighted sequence, 0.7-mm isotropic resolution. Copper sulfate was used as an MRI marker inside reservoirs of ear bars and eye bars of a MRI compatible stereotaxic frame (Kopf) in order to co-register MRI with CT data (iodine can be used as a marker in CT scans, but is not necessary). Timing of MRI scans varied (data not shown) from 6 months prior to headpost implant surgery up to 1.5 years following headpost implant (titanium is MRI compatible but an artifact from the metal will be evident in the scan).

CREATE 3D PRINTABLE DIGITAL MODEL FROM CT DATA

We sought to create a 3D-printed 1:1 replica of a monkey's skull using the cheapest and quickest methods possible for the purpose of surgical planning and forming cranial implants preoperatively. Thus, we used free software wherever possible. All data processing was performed initially on a PC (Windows 7, 3.0 GHz, 6.0 GB RAM) and later performed on other PCs and MacOS machines. There are many options available to convert medical imaging data such as CT or MRI into a digital 3D model. Some tools perform the required steps (briefly, segmenting the desired structure from the surrounding data in each imaging slice, capturing that surface and integrating across slices to generate a 3D surface) almost automatically. McAndrew and colleagues (2012) used Mimics software to generate a digital model of the skull surface. At the time that we initiated these studies, Mimics was quoted at over $20,000 after a 50% academic discount. Lanz and colleagues (2013) used OsiriX software ($699 at that time; currently, free option includes the necessary features, available for MacOS only) to create 3D printable skull models based on CT. Other software options (mostly free and open source) that we vetted but did not use include: Analyze (trial version), 3D-Doctor (trial version), BrainSuite, FreeSurfer, and 3D-Slicer. DeVIDE is an open source 3D visualization and image processing software tool (Botha 2006). Ultimately, we found that DeVIDE worked best for our needs at the time: in addition to being open-source, DeVIDE's graphical interface was intuitive to learn and use (especially given available online tutorials), and performed the required steps quickly and accurately. Other options, including those mentioned, may be just as good if not better than DeVIDE depending on the needs of the individual laboratory. Furthermore, this is a

rapidly evolving field and tools are constantly being developed; for example, the authors have recently begun using InVesalius (free, open-source) for this process with excellent results.

We also attempted to segment bone from MRI data with Analyze and BrainSuite, which could make a CT scan unnecessary. Whereas this was possible using both programs, bone segmentation in MRI was more difficult and required far greater processing time compared to extracting bone surface information from CT scan data. Crucially, results were not completely reliable. Note that new MRI parameters have been shown to provide accurate bone segmentation (Eley et al. 2012, 2014, 2017), however these methods were not available to the authors at the time. In BrainSuite (an open-source MRI processing tool), for example, the outer surface of the bone segmentation from MRI data was good, but the segmentation of bone from underlying tissue was inaccurate, compromising information about the skull thickness. Ultimately, we decided that the additional cost and time of a CT scan relative to an MRI scan was worth the confidence in the accuracy of our 3D model in addition to the ease of software processing. CT also provided information about bone integrity, which was desirable in cases that had been previously implanted with acrylic. For example, it is common for acrylic implants to lead to thinning of the skull underneath the implant that would affect placement of or even delay a subsequent implant. In each case, the most recent CT scan was used to create a 3D model of the skull.

There are several file formats that produce a 3D-printable model. However, STL ("Surface Tessellation Language", or "STereoLithograpy") format is the most widely used and supported format for rapid prototyping. Following the procedures provided in an online video tutorial (Botha 2010), we extracted the surface model of a rhesus macaque skull. With little practice this process can be completed in less than an hour (even faster using InVesalius). Briefly, DICOM files (CT data) were imported into DeVIDE. Thresholds were chosen to segment bone from the remainder of tissue and select only bone in the CT data, then a seed point within the bone was chosen so that only bone connected to that seed remained in the model. Finally, the skull model was exported from DeVIDE as an STL file that could then be repaired and checked in a 3D modeling software as described below.

Cropping and Repairing STL

In order to print the relevant dorsal portion of the skull, STL models were cropped and repaired using MeshLab (free, open source) or NetFabb Basic (free, Autodesk). MeshLab has more advanced functionality but was less intuitive and more difficult to learn. We found NetFabb to be more user friendly and easier to learn to perform the required steps. There are many 3D printing software tools available and tools are being produced or improved upon continuously. Any tool with "STL slicer" and "STL repair"

functionality will suffice. Note that we may have used older versions than what is currently available, but the general steps should be comparable.

We cropped STL skull models in a horizontal plane so that the printed skull replica would have a flat bottom. This was done for two reasons: 1) so that the printed skull would rest on a flat surface to make working with it as a planning tool easier, and 2) to save on cost of printing material, reducing printing costs from 25% to 50%. Apart from the dorsal surface of the skull that is necessary for surgical planning, other anatomical features of the skull are helpful as points of reference. In general, the orbits and auditory meatuses were preserved and used for this purpose. In some cases, a horizontal cut in the STL file parallel to the stereotaxic axis formed by the bottom of the orbits (eye bars) and auditory meatuses (ear bars) was made so that the skull was oriented on the workbench during planning as it would be in the surgery suite. In other cases, a portion of the face and upper jaw were printed so that the replica could be mounted in a stereotaxic frame as with a real head (as in Fig. 3B).

Because the STL is a model of surface geometry created by connecting a point-cloud with lines to generate triangles, any discontinuities in the surface that are created by cuts will result in a zero volume and will render the model unprintable; the surface must be completely closed (termed “watertight” in the industry) in order to obtain a viable print. Holes created upon cutting the model along the desired plane above were closed using NetFabb Basic or MeshLab (this process is much easier in NetFabb). In NetFabb, triangles were added to create bridges and simplify complex holes, and then the auto-repair function was used to close holes. Next, “floaters” were eliminated by selecting the model then inverting selection so that floating or non-connected points could be deleted. NetFabb Basic’s interface makes it easy to determine when the model is a single closed shell, and thus complete and printable. Finally, the model was exported as STL to save all changes. STL does not have a standard system of units, so it is important to note the units used in the original DICOM (e.g., mm) to avoid inappropriate scaling at the time of printing. Using DeVIDE, units are automatically interpreted from the DICOM files and applied to the STL.

PRINTING THE SKULL REPLICA

There are many different types of additive manufacturing (3D printing), which refers to the process of building an object (or “part”) by adding material layer upon layer. The International Standards Organization currently identifies seven different categories of additive processes (ISO/TC 261 2015), that can be loosely classified into three broad groups: solid-based, liquid-based, and powder-based. We used powder and liquid-based printers that were available to us through our campus services and describe the outcome of each below. 3D printing was performed by the Engineering Fabrication Laboratory (EFL;

ZPrinter model 450 powder system; 95-µm layer; 300 x 300 x 450 dpi resolution) through the Engineering Department as well as by the Translating Engineering Advances to Medicine lab (TEAM; Stratasys Objet Eden 260V; 16-µm layer; 600 x 600 x 1600 dpi) through the Department of Biomedical Engineering, both on the UC Davis campus. For our purposes, the accuracy of the 3D-printed replica and therefore the resolution of the printer was our main concern. The ability to draw or mark the replica surface was also convenient for use as a planning tool.

Our first skulls were printed on a ZPrinter model 450 (Fig. 3A and B), a powder-based system where a bonding agent is printed layer-by-layer onto a bed of powder ("binder jetting" process; ISO/TC 261 2015). The powder itself also serves as a support material as the part is built. The 3D replica off the printer is relatively fragile and requires cleaning with compressed air within a specialized hood to remove excess powder. After the part is cleaned, it is bathed in an infiltrant which finishes the curing process and strengthens the replica. A problem with this approach is that if the replica is not cleaned sufficiently, then any leftover support powder will become cured to the print by the infiltrant, decreasing accuracy of the replica. This presents a problem if there are small or fragile features such as previous screw holes, thinning of the skull or protuberances that might be present in an animal previously implanted with acrylic. Also, special attention should be paid to cleaning small crevices, such as the auditory meatus, which is necessary for compatibility with stereotaxic frames, as they can become clogged. Despite these concerns, the resolution of the replica was sufficient for accurate bending of headpost feet prior to surgery. Additionally, the white matte finish surface of this material was easy to mark with pencil during surgical planning (e.g., Fig. 3B).

Several of our skull replicas were printed using the Stratasys Objet Eden 260V (Fig. 3C and D), which is a liquid-based photopolymer printing system ("material jetting"; ISO/TC 261 2015). The Objet Eden 260V uses a photopolymer jetting technology ("polyjet") that can print a variety of materials with different mechanical and optical properties. In contrast to the powder system, this printer extrudes a gel-like support material that is cleaned from the final model with water in a pressure washing chamber. An advantage of this printing system, in addition to superior printing resolution (up to 30 µm accuracy in 16-µm layers), is that the support material does not require an infiltrant and is never inadvertently cured as part of the solid print, so the post-processing steps such as cleaning are not likely to introduce errors. In the case of the Stratasys Objet260, the choice of material will determine the strength and finish of the printed part. In our case, the stronger "VeroWhite" plastic (a proprietary acrylic-based photopolymer) produced a glossy finish which was easily marked with a felt pen that could be erased with alcohol.

Ultimately, both models of printers and printing methods, the binder jetting and polyjet printing systems, were successful for our application. Stereolithography, (SL or SLA, a photopolymerization method) is another common system that would produce acceptable results in most cases. Fusion deposition modeling (FDM, a material extrusion method) is the most common type of 3D-printing system available and is not accurate enough in most cases for this application. Regardless of the printing system, we recommend choosing a printer with a minimum accuracy of 85 μm (300 dpi) based on our experience with the printers described above. Skull replicas from both printers were sterilized with Sterrad gas prior to surgery.

DETERMINING LOCATION OF HEADPOST AND RECORDING CHAMBERS

Headposts are typically implanted well in advance of recording chambers because it can take many months before a primate is fully trained on a behavioral task, which often requires head fixing. Waiting to implant recording chambers in a second surgery reduces the chance of infection and postpones the need for a cleaning regimen. Additional healing time (from 4-12 weeks, discussed below) allows the titanium of the headpost to osseointegrate adequately before attempting to restrain the animal's head. Despite the potentially long period of time between headpost and recording chamber surgeries, it is important to plan recording chamber locations early so that headpost feet do not impinge on future surgical sites, particularly craniotomy locations. However, note that it is possible to remove a headpost foot if necessary, as was done in case #2, at 3.5 years post-implant without complication. Whereas in most cases this planning can be done very roughly (e.g., when all regions of interest are rostral to or caudal to the central sulcus), in some cases it is necessary to plan locations of recording chambers more precisely in order to constrain the headpost location (e.g., when more than one chamber will be implanted). Precise localization of the recording chambers is also necessary when designing an acrylic-free recording chamber because the contour of the chamber will conform to the cranial surface and therefore must be implanted in that precise location (as opposed to the acrylic-embedded recording chamber where the surgeon can choose the exact location of the chamber intraoperatively). In case #1, target locations were determined by using the patterns on the inside of the skull model as a proxy for gyri and sulci; this is a fast solution for determining targets on the cortical surface but not possible for deeper structures (Fig. 3B). In cases requiring more precise localization we used specialized software to determine the location of recording chambers according to structural MRI data.

Monkey Cicerone (Miocinovic et al. 2007a, 2007b) and SPLASh (Stereotactic PLAnning Software) (Sperka and Ditterich 2011) are two software tools developed to guide stereotactic neurosurgery and electrophysiology as well as store anatomical and recording data. Monkey Cicerone software includes a subcortical atlas and SPLASh includes a cortical atlas; both tools are freely available from the respective

authors. In three cases (#3, 4, and 6), targets included cortical areas deep within a sulcus and/or subcortical structures, so we used Monkey Cicerone to identify electrophysiology targets and plan locations of recording chambers. An important feature of this software is the ability to import and co-register MRI and CT scan data, making it useful for planning acrylic-free implants. First, MRI and CT DICOM volumes were imported into Monkey Cicerone software and then aligned and co-registered. Alignment and co-registration were the most tedious steps, but critical to ensure proper positioning of implants and particularly in order to use the included atlas. Once the CT and MRI were aligned, the ear bar and eye bar landmarks in Monkey Cicerone were positioned according to the CT ear bar or eye bar markers described above. In cases where ear and eye bar markers were not visible from scan images or were not aligned properly during a procedure, the CT model was useful in positioning the ear bars in the auditory meatuses and eye bars at the bottom of the orbitals. Although Monkey Cicerone is a powerful tool, it can be difficult for beginners and takes some time to learn.

A major advantage of this process is that one can modify the purchased headpost to best accommodate the location that it will be placed and maximize the number of screws that will be used without compromising the location of future recording cylinders. In our sample, six of nine headposts were positioned rostrally over the frontal bone extending onto the brow ridge. Because of this positioning, the rostral feet of the titanium headposts were shortened to retain two screws per foot, but the length of the headpost feet projecting caudally varied depending on skull size and planned chamber locations. In all five cases using the DAHP-2 headpost (Gray Matter Research, shown bent to fit a printed skull in Fig. 4), at least two screws were kept on at least 5 of the 6 feet, for a minimum of 11 screws per implant (cases #3, 5, 8 & 9) and as many as 14 screws in two cases (#2 & 7). The headpost for case #1 (F, 9.0 kg) was designed to accommodate 10 screws with 1 screw on each of two rostral-most feet that extended lateral from the post, and 2 screws on each of four caudal feet. The headpost design for the three remaining cases (#5, 8 and 9) accommodated 11 screws and was positioned centrally on top of the head.

BENDING HEADPOST FEET TO CONFORM TO THE SKULL SURFACE

A primary goal was to pre-fabricate implants in order to decrease risk of infection and other complications related to surgery duration. To decrease surgery times and maximize osseointegration potential, titanium headpost feet were bent to conform to the 3D printed skull replicas as closely as possible prior to the surgery. Our goal was to maximize points of contact between titanium and bone with no more than a 1-mm gap between the implant and the skull at any point. This target was attained in all cases with the use of the 3D printed skull replica. For case #1, a footed headpost that fit precisely to the skull surface was machined from the titanium alloy Ti-6Al-4V using the 3D-printed skull replica as a

template. In five cases (#2, 3, 4, 6 and 7), the double asymmetric headpost (model DAHP-2, Ti-6Al-4V) from Gray Matter Research was implanted. In the remaining three cases (#5, 8 and 9), a custom footed headpost was made that could accommodate an eye coil connector. With the exception of case #1, all headpost feet required manual bending to conform to the dorsal surface of the skull.

Foot bending can take up to 6-8 hours depending on the skull contour and the experience of the individual doing the bending, therefore it is not recommended to make further adjustments during surgery unless necessary. There is a point of diminishing return towards the end-stage of bending the metal where a small correction in one area will lead to multiple corrections that need to be made elsewhere. In two cases of mature male NHPs who had previously been implanted with acrylic implants, it was necessary to remove small irregularities on the bone surface to achieve a suitable fit. In both cases this procedure was practiced on the skull replica during the planning stage. To bend the headpost feet, bending bars were wrapped with self-adhesive bandage to enhance comfort in the hand as well as allow the bending bar to be clamped securely in a bench clamp. Clamping the bar and holding the headpost to guide each movement allowed for better control and made frequently checking fit against the skull replica more efficient. Each headpost foot was bent using small incremental adjustments (large or repeated bends risk cracking the metal) starting proximal to the post and moving distally. Note that headpost feet can be bent up and down and rotated slightly but not bent side to side. Feet were bent between screw holes as much as possible in order to avoid deforming screw countersinks, which could cause a screw not to seat well, potentially leading to irritation of the skin above it. Headpost feet were cut to length between screw holes using a Dremel cutting wheel and then deburred using a sanding wheel attachment.

ESTIMATING SCREW LENGTHS PRIOR TO SURGERY

An important consideration in acrylic free implants is the length of each of the individual screws. In traditional acrylic implants, bone screws are screwed in only partially so that most of the screw protrudes from the skull to serve as an anchor for the acrylic, and so the screws are much longer than the thickness of the bone. In acrylic-free footed implants, however, the screws must be fully seated in the implant to avoid irritation of the skin above the implant. The screw must also be long enough for the threads of the screw to extend through both the outer and inner cortical tables of the skull in order to maximize the strength of the connection between the skull and implant. Ideally, it should be no longer, minimizing contact with the dura mater (see Adams et al., 2007, Fig. 3). For these reasons, we chose to use Gray Matter screws designed for use with their headpost ($20 each). Gray Matter bone screws are made of titanium (Ti-6Al-4V) with flat tops that seat fully into the headpost countersinks and do not protrude above the feet, minimizing irritation to the overlying skin. Further, they are micro-blasted to improve

osseointegration and have a short rounded tip (0.1 mm) beyond the threaded length of the screw so as not to damage the dura mater as the threads extend almost completely to the end of the screw.

The appropriate lengths of each screw were estimated prior to surgery to ensure that the correct number and length of screws were prepared, saving significant time in the operating room. We estimated skull thickness in a DICOM viewer (e.g., RadiANT) with measuring tool function – screw locations were estimated by eye in the software based on observation of the bent headpost on the skull replica, and measurements at several locations across that region were taken to obtain average skull thickness measurements as well as minimum and maximum possible thicknesses that would constrain screw length choices. In some cases, skull replicas were drilled and a depth gauge used to measure skull thickness with more precise localization of screw position (using this method, one can also take into account the spacing between the skull and headpost foot). Because the length of the Gray Matter screw is measured from top of the threads to the screw tip, the appropriate screw length is the skull thickness plus 0.1 mm for screw tip plus an estimate of the spacing between skull surface and headpost foot. For example, if skull thickness is measured as 3.0 mm, then a 4.1 mm screw was chosen because a 3.1 mm screw would be too short for the threads to extend through the inner table if there was even a 0.1-mm gap. A record of screw length predictions, as well as extra screws of each length, were packed for surgery. A depth gauge was used during surgery to verify proper screw lengths.

SURGICAL METHODS FOR HEADPOST IMPLANT

All animal procedures were approved by the Institutional Animal Care and Use Committee (IACUC) at UC Davis and conformed to AAALAC, NIH, and Society for Neuroscience standards. While specific procedures varied from case to case, all animals were sedated with intramuscular ketamine followed by placement of an intravenous catheter, then intubated and anesthetized with 1-3% isoflurane. Heart rate, blood oxygenation and rectal temperature were monitored continuously throughout each procedure. The surgical area was shaved and prepared with povidone iodine solution and a sterile field was established with a sterile drape under aseptic conditions. The time of first incision was noted, marking the beginning of the surgical procedure.

In four cases a midline incision was used, and in five cases the skin was incised following the “U-flap” guidelines suggested by Gray Matter. Briefly, a U-shaped incision was made beyond the area of the implant footprint. Blunt dissection was used to separate the skin and fascia from the surface of the skull. The skin flap was kept moist with sterile saline soaked gauze throughout each procedure.

Once the periosteal surface of the skull was exposed and cleaned, the headpost was positioned and the fit was checked. In most cases the headpost fit on the skull exactly as it had on the replica without needing additional changes. In cases #3 and 4, slight adjustments were made to headpost feet with the bending bars only as necessary, adding 10-15 minutes to total surgery time. In these two cases, irregularities in the bone surface were carved away using a bur and pneumatic dental drill so that the headpost seated more fully onto the skull surface and increased contact between bone and titanium. The headpost was placed in its final location and two of the most proximal holes were marked with a pencil, then the headpost was removed and those two holes were drilled. Before attaching the headpost to the skull, a layer of Fusion Bone Putty (hydroxyapatite mixture; described below) was applied to the bottom of the post feet and to the skull surface to fill any gaps. The headpost was attached with first two screws (but not tightened completely) and then remaining holes were drilled with the headpost in place so that all holes were drilled in the correct location. Drilling screw holes properly takes practice and skill (the skull replica can be used for this purpose; it is also customary to practice using a mature coconut). Drilling must be performed with a quick, smooth motion to avoid excessive heat build-up that could damage the bone, and perfectly perpendicular to the skull surface so that the screws will seat completely into its countersink. We used both a pneumatic dental drill as well as a hand drill (see below), and both worked well. When using a pneumatic drill the sterile surgical assistant continuously infused the skull where the hole was drilled with sterile saline. This aided in visibility as it washed away the bone dust, as well as keeping the tissue from overheating. Screw holes were drilled using a 1.8 mm diameter carbide bur (SS White Burs, Round #6), which is slightly smaller than the 1.9 mm core diameter of the Gray Matter bone screw so that the screw could be used as self-tapping, ensuring maximal contact between screw surface and bone. Despite measuring within software for screw lengths prior to surgery, actual depths were measured with a surgical depth gauge to ensure the correct length of screw was used. This verified that the estimates were largely correct, although in a few cases a different length of screw was substituted. Fusion Bone Putty was applied to each screw before insertion, and added around the edges of the headpost feet, filling any gaps and crevices. Finally, screws were tightened by hand with a 1.3 mm hex driver (Gray Matter), alternating about quarter to half turn of each screw, until all screws were just seated in the headpost. This reduces the risk of over tightening the screws and stripping the hole and potentially damaging the bone.

The retracted muscle and fascia were then pulled over the feet and sutured whenever possible in order to put tissue between the feet and the overlying skin. This was not achievable in some cases where an animal had a previous acrylic implant, or for regions very close to the midline. For midline incisions, the scalp was sutured with simple interrupted stitches so that the skin was closed around the implant as tightly as possible. In cases in which a U-flap was made, the location of the post base incision was estimated and

marked with surgical marker on the skin surface before cutting the flap. After the headpost was screwed to the skull, the skin was stretched forward and the hole was cut at this time in order to position the hole correctly at the base. To limit skin retraction, we retained as much tissue as possible while cutting this hole: A small "X" incision was made in the location where the base of the headpost would protrude from the skin. The skin flap was stretched forward until the top of the headpost met the "X". While holding the flap in this configuration, the "X" was opened further with a scalpel just enough to accommodate the post and then the flap was pushed down over the post (widening the incision as necessary) to the surface of the skull and headpost feet. The margin from the X incision was trimmed with a scalpel. The U-flap was closed with simple interrupted sutures. All other surgical and post-operative procedures were as per usual surgical guidelines as referenced above.

USE OF HYDROXYAPATITE TO AID OSSEOINTEGRATION

In contrast to traditional screw-fixed acrylic implants, the fixation method for titanium footed implants is via osseointegration (as described above) which is enhanced with the application of a hydroxyapatite (HA) coating or paste. Similar studies have used an HA paste (Adams et al. 2011) or HA coating applied to the titanium surface in contact with bone (Lanz et al. 2013) to increase osseointegration of the implant. We searched for alternatives to the [human-grade] Mimix QS (Biomet) HA paste used by Adams and colleagues (2011) due to high cost of the material ($884 for 3.45 cc). We weighed different options and decided to use Fusion Bone Putty (Veterinary Transplant Services, $68 for 1 cc single use vial; see Table 3.2 for details) in almost all of our implant procedures. Fusion Bone Putty is a mixture of HA, demineralized bone matrix (DBM) and beta-tricalcium phosphate (β-TCP), which are necessary ingredients for bone growth; DBM and β-TCP increase the rate of osseointegration compared to just HA alone (Urist et al. 1987; Trisi et al. 2003). Fusion Bone Putty single-use sterile packs (1-cc or 3-cc vials) have a long shelf-life (2 years) at room temperature. We found that the 1-cc vial of bone putty was ample for a single headpost surgery. In the event that a drilled hole could not accommodate a screw (one occasion of a mis-drilled hole) the hole was packed with bone putty. Small defects (< 1 cm diameter) apparent in the bone from previous implants (e.g., old screw holes not fully healed) were filled with bone putty as well. In addition to the use of Bone Putty, an HA coating was applied to the footplate of the headpost in one case (#9) prior to implant (PCS Materials; ~$500) with the hope that the HA coating on the superior surface of the feet would prevent skin recession (see Results and Discussion).

ATTACHING THE HEADPOST TO THE PRIMATE CHAIR

It is important to wait a sufficient amount of time for osseointegration of the headpost before attempting to first attach the headpost to the primate chair. Osseointegration of titanium load-bearing implants takes

6-12 weeks (Hacking et al. 2012). Hacking and colleagues (2012) waited 6 weeks before head-fixing a subject after implantation of a titanium headpost surface-treated to optimize osseointegration. Adams and colleagues (2007) waited two weeks with a similarly treated post. In another case, Adams and colleagues (2007) waited just 12 days after surgery to use the headpost, but after just 6 days of use this headpost (Crist Instruments) failed at the welded post-footplate juncture (note that all of our headposts were from a machined from a single piece of stock and were not welded) and the footplate remained implanted (this event was unrelated to early posting). Inspection of this titanium footplate 1 month after implantation showed considerable remodeling and development of desired "woven bone" callus formation at the edges of the titanium footplate and around the tips of screws on the inside of the skull (see Fig. 5 in Adams et al. 2007) supporting the idea that 6-12 weeks is more than sufficient and likely overly cautious. In order to allow sufficient osseointegration, we waited a minimum of 4-5 weeks before attempting to use headposts, and as many as 12 weeks in cases of larger, stronger animals and/or if there had been complications with previous acrylic implants that might compromise bone integrity. Age of the animal was also a factor in estimating healing times – we waited longer than 12 weeks in the case of a geriatric animal (age 29.3, or ~88 human years). Refer to Table 4 for post-implant latency to the first head fixing where available. We used the healing period to gradually acclimate novice animals to the laboratory environment and headposting procedures.

A disadvantage of the footed headpost is that the angle of the post is determined by the location on the skull where it fits best and does not necessarily project vertically from the skull relative to the primate chair as it often does in an acrylic implant where the post orientation can be determined more precisely by the surgeon. Consequently, in many cases the angle of the acrylic-free post does not readily mate with a standard primate chair (e.g., Crist-style primate chair) which has a vertically-oriented head holder. Care was taken to center the post as much as possible, so only pitch (and not yaw or roll) axis of rotation would need to be adapted to the chair, but in reality, a system with three axes of rotation is necessary to ensure that the fixed posture of the animal's head is both comfortable and compatible with the experimental setup. We used a system of post and strut clamps as shown in Figure 5 (Misumi, see Table 3.2 for details) to attach the headpost holder to the primate chair. Approximately 10 cm of the distal end of the headpost adaptor was turned down on a lathe to a diameter of 12 mm in order to mate the Gray Matter headpost adaptor to the strut clamp. Alternatively, clamps with different diameters may be available through Misumi as a custom order. The clamps were adjusted in order to optimize the animal's head position and maximize the animal's comfort. An advantage of this system is that the angles can easily be adjusted in small increments. Once the optimal position is determined, the clamps were tightened and one system of three pieces was reserved for each animal. The Misumi clamps are small and inexpensive enough that it is

efficient to have a single set for each animal-chair combination and avoids the need to reconfigure the clamp system during each recording/behavior session. In the case of one large male macaque, one of the clamps had to be modified by adding a set screw to further tighten the clamp for recordings. In our experience, clamps that require daily tightening will need to be replaced approximately once every 3-4 years due to wear of the ratcheting clamp levers.

At the time of this writing, Gray Matter has developed an articulated clamp head-holder system that solves the problem of the implant protruding from the head at variable angles and includes measurement scales engraved onto the hardware so that configurations can be reproduced reliably. The articulated clamp system ($1500) is designed to mate with their new primate chair and docking station (prices available upon request). While Gray Matter's clamp may be compatible with other chair designs, it does not appear to be compatible with our Crist primate chairs (audio or vision style chairs). Crist Instruments also has a solution, the "swivel head positioner", that can accommodate a variety of head post angles, and should work in most cases.

IMPLANT MARGIN CARE

In each case, implant margin condition was monitored at least once per week. In the best of 9 cases, the implant margin remained clean and dry and no maintenance was required for the 1.6 years that the headpost was implanted (case #3). If granulation tissue or evidence of weeping or exudate was observed, then the fur at the implant margin was shaved once per week and cleaned gently with a solution of either betadine or chlorhexidine. Topical application of silver sulfadiazene was applied 3-5 times per week in cases with excessive weeping or exudate.

3D PRINTED HEADPOST COVERS

Primates naturally engage in grooming behaviors and may exhibit a tendency to pick their sutures or implant margin, particularly while they are healing and cannot be pair-caged with another monkey. Animals are provided extra enrichments such as puzzle toys filled with popcorn and fruit to mitigate this behavior. Once they recovered sufficiently from surgery they were paired with a companion daily, which further prevents potentially self-injurious behavior. As discussed in more detail below, the skin at the implant margin of the titanium headposts had a tendency to recede along the implant feet, exposing metal and screws. We were concerned that potential irritation would promote scratching and picking at the site and exacerbate skin recession. To limit the monkeys' ability to access the implant margin we designed customized covers ("hats", see Figure 7) that were then 3D printed with acrylonitrile butadiene styrene (ABS) plastic and customized to each animal.

The hats were designed to cover the exposed portion of the headpost in addition to protecting the implant margin and area of skin covering the implant. Whereas the hat brim needed to be close enough to the scalp to prevent picking, air flow is needed to prevent the proliferation of anaerobes; we therefore aimed for approximately 5 mm spacing between the scalp and brim. Initially, we designed the hat to screw in to the top screw similar to the provided Gray Matter cover (Fig. 7A). However, we found that the hats had a tendency to spin which would wear down the top portion of plastic very easily. We updated our design to screw from the front using the same screw hole that is used to attach the headpost connector. This "igloo" design (Fig. 7B and C) solved the spinning problem and was much more robust. We printed the hats with excess material around the brim and then removed material with a sanding belt and various sandpaper grits to customize the fit and create a smooth finish. Adjustments were noted and the CAD file (Autodesk Inventor) was updated for future iterations. This method of rapid prototyping was very useful for this purpose and small adjustments could be made easily and cheaply in order to achieve a highly functional part.

DESIGN AND PRODUCTION OF THE PEEK RECORDING CHAMBER

In addition to titanium footed headposts, in one case (#3) we designed a custom-fitted recording chamber similar to previous reports (McAndrew et al. 2012). The recording chamber location was planned using Monkey Cicerone software. Once MRI and CT images were co-registered and aligned (as described above a chamber template was chosen in Cicerone with the correct inner diameter (17 mm). Our recording chamber was designed to fit a 17-mm Crist grid and grid adaptor to mate with a Narishige hydraulic microdrive (model MO-95). We used Monkey Cicerone's electrode tracker functionality to maximize access to our region of interest and estimated grid positions and recording depths (Fig. 6A). Cicerone provides stereotaxic coordinates, however it was not possible to export Cicerone's coordinate system to communicate with CAD software directly. Thus, the positions of the two ear bars and one eye bar were used to define a reference plane. The chamber bore was oriented parallel to the sagittal plane, so its position was defined by translation in two dimensions (lateral and caudal) and one angle that was measured from the stereotaxic reference plane using a screenshot taken from Cicerone. This position information was used to determine the location of the chamber in Meshmixer (Fig. 6B). Then the area of skull directly below the recording chamber was isolated in Meshmixer, along with reference points corresponding to ear bars and one eye bar, and the resulting STL was imported into Autodesk Inventor (Fig. 6C; this step is to limit the amount of system resources needed to work with the STL in Inventor). A "User Coordinate System" was established in Inventor to aid in generating the chamber in its proper location with the origin at the surface of the skull at the center of the chamber, and the X vector pointed along the bore of the cylinder (the direction of the electrode track as defined in Cicerone; Fig. 6C). A

chamber was then generated by extruding a ring along the X axis and centered at the origin. The extrusion was terminated on the STL surface, creating a cylinder with a base that conformed perfectly to the skull contour. Feet were then added at desired locations, such that they were normal to the center of their mounting hole location. The four feet of the chamber were designed with curved edges in an attempt to minimize irritation to the skin above. Prototypes of the chamber were 3D-printed and positioned on the 3D-printed skull replica at several stages of the design process to verify positioning and fit. The final recording chamber was 3D-printed from PEEK by Solid Concepts (Austin, TX) using a selective laser sintering process. A copy of the recording chamber was printed in VeroWhite (Stratasys Objet260 printer) and truncated with a Dremel cutting wheel to only include the base and feet (~5 mm height) and served as a template for marking the implant position on the skull and performing the craniotomy during surgery.

IMPLANTING THE RECORDING CHAMBER

The 3D-printed PEEK recording chamber was steam sterilized and implanted following all previously stated surgical procedures. We used a U-shaped incision as described above for headpost implants. The recording chamber fit precisely as planned and the desired location was easy to find as there was only one way that the chamber base could be matched with the skull. The chamber's outer perimeter and screw hole locations were marked with a surgical pen. The shortened 3D-printed implant template (Sterrad gas sterilized) was used to mark the inner boundary of the recording chamber and the craniotomy was performed with a surgical drill. This would have been difficult given the height and angle of the chamber. The first hole was drilled, then the implant was attached with one screw, then the remaining three holes were drilled with the implant in place. Holes were initiated using a sharp drill bit (Veterinary Orthopedic Implants, $35.00) held with a hand tap handle (Veterinary Orthopedic Implants, $115.20) in order to ensure accuracy of positioning and limit heat build-up. Finally, a surgical drill with a bur was used to complete the holes safely without risking damage to the dura. The bottom surface of the implant and the skull surface were coated thinly with bone putty. The three remaining titanium screws (Gray Matter) were tightened, alternating about a half turn per screw. Screws fit very tightly and were screwed until the base of each screw was just seated in its respective countersink to avoid stripping. The chamber was filled with sterile saline to determine if there was a water-tight seal and leaks were addressed by packing Fusion Bone Putty around the outer edge of the bone-implant interface. Fascia and muscle were pulled over the skull and implant feet and sutured wherever possible as described above for the headpost. The skin flap was pulled over the implant and an X-shaped incision was cut for the chamber to fit through. The skin flap was sutured and skin glue was placed over the sutures. Chamber positioning was later verified using MRI, before physiological recordings commenced.

RECORDING CHAMBER LEAK TESTS

In addition to routine recording chamber maintenance, leak tests were conducted regularly to ensure that a water-tight seal remained at the implant-bone interface. A leak test was performed at least once per week during cleanings by filling the chamber with fluid and noting the level of fluid after 15 minutes. For the lifetime of the implant (see Results) the fluid level remained stable at each leak-test, indicating a watertight seal was achieved and maintained.

Because case #3 had a history of infection, we designed a cover for the recording chamber to prevent the monkey from being able to pick at the implant margin that was similar to the "hats" fashioned for the headposts. The cover was a two-piece design which fit over the Crist chamber cap snugly and utilized the flat edge of the cap to prevent rotation of the "hat". The chamber cover was 3D printed and excess material around the brim was sanded down for a custom fit so that it would not touch the scalp at any point.

RESULTS

SURGERY TIME SAVINGS AND COST EFFECTIVENESS

The feet of a titanium headpost were bent to conform to 3D printed replica skulls prior to surgery, leading to a better overall fit and dramatically reduced surgery times (50% to 70% time savings) compared to traditional methods. Our acrylic-free headpost implant procedures averaged 1 to 2 hours compared to 2.5 to 3.5 hours for acrylic-embedded headpost surgeries performed by the same surgical teams. Bending the titanium feet prior to surgery was a significant improvement over bending the feet intraoperatively, as has been previously reported (Adams et al. 2007). Intraoperative bending of a titanium footed headpost to fit a skull can take several hours. In our cases, pre-operative bending took from 6 to 8 hours, depending on the complexity of the skull (for example, bending an "S" curve to match a prominent brow ridge presented more of a challenge). Furthermore, while this is a considerable time investment, we were able to achieve a very close fit (1-mm gap maximum, compared to 2-mm gap, Adams et al. 2007) to increase osseointegration, even by individuals bending the feet for the first time.

DURATION OF HEADPOST IMPLANTS AND OUTCOMES

The outcomes of the headposts that were implanted using these techniques are summarized in Figure 8 and Table 4. Five of these animals are still implanted, while the other four were euthanized due to study endpoints (3 animals) or due to reasons unrelated to the implants or experimentation. There were no complications or cases of infection that compromised the integrity or functionality of the implant in any of the 9 cases, which includes two animals with histories of chronic infection associated with prior acrylic

implants. One case (#2) has been implanted for over 4 years. Several cases have undergone surgeries for recording chambers or other repairs, and investigators have observed growth of bone along the sides of or covering headpost feet, indicating osseointegration consistent with previous reports (see e.g., Adams, et al., 2007, Fig. 7 or Adams et al., 2011, Fig. 5). This is in contrast to the results from 11 acrylic implants (dental resin or orthopedic cement) reported in Lanz et al. (2013). In their hands, the average time that the implant had integrity was 8 months (range 3 – 12 months), with two cases where the implant had to be removed due to infection and three additional cases where the device was explanted for other reasons (i.e. breakage). This contrasts with this report, where the implant remained fully functional in all monkeys until euthanasia (a minimum of 2 years for all monkeys still participating in experiments) and no cases of infection or the necessity to explant.

IMPLANT MARGIN CONDITIONS WITH FOOTED HEADPOSTS

Adams and colleagues (2007) emphasized that the implant margins of their titanium headposts did not require maintenance or cleaning "throughout the lifetime of the implant." In contrast, Mulliken and colleagues (2015) assert that footed implants result in "skin recession [which] can lead to exposed bone, which can degrade over time, and also increases the likelihood of an infection as granulation tissue proliferates, jeopardizing the integrity and lifetime of the implant." Across our 9 cases we found considerable variability in the need for cleaning or treatment; Figure 8 summarizes implant margin conditions for all nine cases. In 7 of 9 cases, retraction of the skin and exposure of titanium feet occurred; metal exposure occurred as early as day 30 in case #9 and as late as day 314 in case #8. The implant edge around case #4's headpost remained clean and dry and required little to no cleaning until he was euthanized for unrelated health issues at the age of 30.8 years. Case #2 continues without metal exposure. We compared outcomes across the type of incision (U-shaped vs. midline), whether there was previously an acrylic implant in place, surgeon, type of headpost implanted or other factors (Table 3) and found no consistent differences across cases. Cases with skin retraction were treated with frequent cleanings and application of silver sulfadiazine ointment as noted above in Methods. In three cases we attempted surgical intervention by pulling skin over the feet and suturing it closed, however in each case the scalp quickly regressed to its original state. Despite the frequency of skin retraction (78%), we observed no cases of bone exposure. The lack of bone exposure in all of our cases is in stark contrast to Mulliken and colleagues' (2015) assertion that bone exposure is an eventual outcome of using this style of implant. In our cases, the skin retracted only along the titanium feet, and the skin overlying the bone remained fully intact and well adhered to the underlying bone. Thus, as opposed to a circular or oval retraction as described by Mulliken and colleages (2015), in our experience the skin edge took on a scalloped shape, with good adherence to the skull but retracted along the titanium feet. In one case, skin regression seemed

to be due to irritation from the tops of the screws themselves; in this case (#6) two screws were eventually ejected. For each screw ejection, granulation tissue filled the site and the skin regrew to cover the foot and empty screw hole within a two-month period. Furthermore, as the implant osseointegrates and bone grows over the feet, the skin grows with the bone. There were no cases of peri-implant infection or other complications for years from when skin recession was first observed (Fig. 8 and Table 4).

Recording Chamber Outcome

The 3D-printed PEEK recording chamber in case #3 maintained a watertight seal from 1 week post-implant (first cleaning) until the implant was removed 10 months later. The PEEK implant edge remained clean and dry with minimal maintenance for about two months after which granulation tissue appeared, but the skin did not recede from the implant margin. After 3.5 months the recording chamber could be moved slightly with some manual pressure, indicating that the tightness of fit was beginning to be compromised, but it remained watertight and free of infection for several more months. At 8.5 months the caudal medial screw of the PEEK recording chamber fell out and the chamber became much looser, but still remained watertight. The case was assessed via CT scan and consult with a radiologist, confirming osteomyelitis and loss of bone under the caudal portion of the implant. It is worth noting that the portion of skull that became infected under the PEEK implant was an area of bone that had regrown after a previous case of osteomyelitis under an acrylic implant. The recording chamber was promptly removed and the animal recovered without incident. His titanium headpost remains intact and fully functional and the animal continues to participate in psychophysical experiments.

Single neuron recordings were performed through this recording cylinder, using the same techniques as with a traditional Crist cylinder. There was no noticeable difference in the ability to maintain single neuron isolation, operation with the Microdrive, or any other aspects compared to the previous techniques, indicating that the cylinder was as stable as a titanium or stainless steel cylinder.

Discussion

Headposts

In nine rhesus macaques, we implanted titanium footed headposts that were formed prior to surgery to conform to a 3D printed skull replica based on CT scans of each animal's head. A major benefit of pre-forming the implant is that it is possible to achieve a closer fit between the implant and skull surface. Minimizing the distance between the bone and implant and maximizing contact points leads to a more stable interface between the bone and titanium and faster and better osseointegration (Plecko et al. 2012).

A second major advantage of implant prefabrication is that it reduces surgery times up to 70%, which translates to decreased risk of infection and complications (Mangram et al. 1999; APIC 2010). Additionally, this can reduce cost (surgical suite recharges, veterinary staff, etc.), if applicable. This is based primarily on the amount of time it takes to accurately bend the titanium feet to fit snugly against the skull, in our experience taking 6-8 hours. A well-experienced individual may be able to perform this task in considerably shorter amount of time, which could be appropriate for large laboratories where many surgeries are performed each year, but is less desirable for smaller laboratories where individual investigators may do only 2-3 surgeries during their training period. Again, the close fit with minimal gaps and the majority of the feet firmly against the skull will allow for maximal osseointegration. Finally, if a surface treatment is to be applied to the headpost, such as a HA coating, it would be preferable to perform bending prior to treatment for best results. A second consideration is the use of titanium versus ceramic screws. Titanium has the advantage of the osseointegration, but a clear disadvantage that it will produce a considerable shadow in MRI and fMRI images. If the brain region of interest is several millimeters away from the screws, this should not present a problem. However, the titanium headpost produces a large shadow in MR imaging as well, so the slight reduction from the ceramic screws is less of an issue. Alternatively, ceramic screws in an acrylic-based implant serves the same purpose as the titanium screws, although they tend to be more expensive.

A persistent issue we encountered with the acrylic-free headposts was retraction of the skin at the implant margin and exposure of the titanium feet (Fig. 8). This was unexpected because previous reports have claimed that the titanium headpost implant margin remained intact, clean and dry and required little to no maintenance (Adams et al. 2007; Lanz et al. 2013). Other reports of acrylic-free implants describe skin recession as a minor consequence without discussion of extent or progression of recession (Pfingst et al. 1989; McAndrew et al. 2012). Yet another recent report claims that footed implants lead to skin recession with bone exposure as an eventual outcome (Mulliken et al. 2015, Fig. 1). The extent of skin recession varied from none at all to approximately 14 mm of skin recession (two screws exposed) along several feet, with the exposure of several screws in the most severe case. No single factor (age, previous acrylic implant, etc.) was consistent to explain why this was more of a problem in some animals than in others (Table 4), although the sample size is too small to make definitive conclusions. There was no difference between the midline and U-flap procedure in our hands. This is somewhat surprising as the U-flap procedure is intended to avoid dehiscence and skin retraction because after surgery the feet of the post are entirely covered by intact skin and the sutured “U” incision falls outside of the footprint of the headpost. We also considered whether direct contact between the implant feet with the skin, or with intervening fascia or muscle made a difference, but we were unable to determine that definitively as all surgeons

attempted to cover the implant feet with as much tissue as possible, and it was difficult to assess the extent post-operatively. Despite this variability, we did not find a single instance of bone exposure, the skin always retracted directly above the titanium implant and even in cases where more than one of the titanium feet was exposed, the skin did not retract between them, giving the skin margin a scalloped appearance. Finally, after considerable care and veterinary attention, we concluded that exposure of the titanium feet of the implant was not of great concern because the implant margin would stabilize and there were no clinical concerns or negative outcomes such as infection due to the exposed metal.

While finding that metal exposure is not a specific concern in itself, the risk for infection is increased whenever there is a breach of the skin. Skin recession at the implant margin requires frequent monitoring, cleaning and treatment when it occurs. An ideal implant technique would support adhesion of the skin tissue to the implant at the appropriate junctions without compromising osseointegration of the implant with the bone. This is the main challenge of bone-anchored percutaneous implants and is an active research area in the application of human prosthetics extending beyond cranial implants in experimental animals. Poor epithelialization at the skin-implant margin leading to infection is a common problem with percutaneous osseointegrated prostheses (POP), a technique that allows a prosthetic limb to be anchored directly to the bone via a titanium rod (Holt et al. 2013; Pitkin 2013). Dental implants have provided the model for percutaneous implant development in humans as well as in NHP, however, dental implants have decreased rates of infection compared to POP implants because the gingiva surrounding dental implants epithelializes faster than non-oral epithelial implant interfaces (Pendegrass et al. 2015). Furthermore, whereas roughening the titanium promotes better osseointegration, Pendegrass and colleagues (2008) found that a smoother surface of the Ti-6Al-4V titanium alloy contributes to faster and better epithelialization *in vitro*, suggesting that polishing the upper surface of the titanium feet would lead to better implant margin results in the NHP headpost. Different coatings and treatments of the titanium implant surface, such as with HA or fibronectin have also been demonstrated to improve epithelial cell (fibroblast) adhesion (Chimutengwende-Gordon et al. 2011). These findings suggest that devising a cost-effective methods for coating the implant after it is formed and before it is implanted would improve the adherence of the skin and reduce retraction of the implant margin in titanium NHP implants.

The nine cases reported from three laboratories in the current study is the most extensive account of acrylic-free titanium headposts and implant margin outcomes to our knowledge. The nine cases presented here represent both sexes and range considerably in age and weight. Five animals are still implanted with titanium footed headposts and continue to be enrolled in experiments, with the longest headpost implant surviving over 4 years to date. Not a single case of the 9 studies showed any signs of bone exposure,

infection or other complication that would require removal of the implant, and all headposts have remained stable since the time of implantation.

RECORDING CHAMBER

We designed a customized recording chamber using structural MRI to guide positioning and CT data to form a perfectly contoured implant. The recording chamber was 3D printed in PEEK and implanted onto the skull of case #3 with four titanium bone screws. Using this method resulted in a perfectly placed and fitted recording chamber that remained watertight (leak-free) for 8.5 months. The recording chamber was placed partially overlapping a region of bone that had regrown after becoming infected under a traditional acrylic implant. Despite having been able to heal for nearly two years (693 days), the infection returned to the same site of the skull, compromising the implant. Recurrence of osteomyelitis after a prolonged remission is a commonly recognized problem in the human literature (Donati et al. 1999; Uçkay et al. 2006; Stevens et al. 2007; Yun et al. 2008), so much so that a recent report stated that "'cure' of the disease cannot safely be declared" (Panteli and Giannoudis 2016). Whereas recurrence of osteomyelitis often occurs even in the absence of a new trauma or apparent route for reinfection (Donati et al. 1999; Uçkay et al. 2006; Stevens et al. 2007), the problem is particularly salient for veterans who have sustained wounds in combat and for whom the presence of an orthopedic device is a major risk factor (Yun et al. 2008). Considering this, we believe that the return of bone infection was not intrinsically due to the procedures stated in this report, although re-implant in the affected area may have contributed to reactivation of the infection. Ultimately, the question remains whether an implant can be safely placed over a previously infected region of bone, and if so, what are the best procedures to follow to prevent re-infection. It should be noted, however, that this is not a problem for implantation into bone areas that were never infected, as this same animal has a non-acrylic headpost that has remained infection free for over 4 years to date.

COMPATIBILITY WITH EXISTING SYSTEMS

Compatibility of implant hardware with head-holders and recording systems is an under-appreciated and under-communicated issue in NHP studies. For example, the headpost must be designed to mate with a head-holder which must be secured in some fashion to the primate chair or an external apparatus. Similarly, the recording chamber must accommodate recording or stimulating hardware such as a microdrive, which in turn is often constrained by the specific style of electrode being used. All these considerations (primate chair, recording set-up, stimulus presentation, electrode style, etc.) must be taken into account when deciding upon or designing any component. The three labs in the current study had all previously used a Crist-style headpost system to mate with Crist primate chairs built for visual or auditory

studies. Two labs used Misumi clamps (Figure 5) to adapt headposts to the chair and accommodate various angles. The third lab designed their headpost to mate directly with a custom headpost adaptor and they modified the primate chairs directly to accommodate the headpost angle by replacing the top bar. There are commercial alternatives, for example from Crist Instruments and Gray Matter, which perform similar function but at considerably higher cost. However, we did have to modify the Misumi clamps to add a set screw for extra stability for the largest animal, so it may be prudent to consider those alternatives for particularly large or aggressive animals. Finally, the recording chamber was designed specifically to be compatible with a Narishige hydraulic microdrive.

The major advantage of the 3D-printing described here is that it is possible to design and test specialized parts quickly and inexpensively. For example, one can place the replica with a headpost into the chair to verify that adaptors for recording cylinders, electrode holders, microdrives, pre-amplifiers, etc., are appropriately positioned before involving the NHP. Others have fabricated custom headposts and cylinders without the replica, milling the hardware directly from the computerized software (Logothetis et al., 2002), although this requires a sophisticated milling machine (in this instance a 5-axis Willemin W428) which is not available to most laboratories. Alternatives are commercially available custom cylinders (i.e. Rogue Research; Johnston et al., 2016) which should be considered, as they also produce the 3D replica but cost on the order of $1500. Other commercial (e.g. Crist Instruments), institutional or independent machinists can also custom fabricate such cylinders, although they also tend to be expensive (range $1500 - $5000 from our quoted estimates). In contrast, the 3D printed PEEK cylinder was on the order of $150-$200 to print the cylinder plus ~$150 to design the cylinder based on the position on the skull. Given that the tolerances of 3D printing (+/- 0.25 mm) has sufficient resolution and there are considerably lower forces on recording cylinders compared to headposts, the cost drove our decision. It should be remembered, however, that unlike titanium, PEEK does not osseointegrate. Rapid prototyping technology, both 3D software tools as well as additive manufacturing or 3D printing hardware, is rapidly advancing. In the five years since we began this project, significant improvements have been made, and we discuss these changes in Methods where applicable. Regardless, the general methodology we described will be relevant for some time. Advances in manufacturing and 3D modeling will undoubtedly continue to help overcome barriers in creating implants in a variety of materials that are customized to the patient or research subject. We hope that this and similar results will promote discussion and research so that we can further refine implant methods for NHP research.

CONCLUSION

Despite the increase in popularity of acrylic-free methods and the use of more biocompatible materials, the use of acrylic for NHP implants remains the most commonly used choice. A potential hurdle in the adoption of acrylic-free methods may be increased cost compared to acrylic, as well as uncertainty regarding techniques, timelines, and outcomes. We implanted nine acrylic-free titanium footed headposts, and one PEEK recording chamber. Our primary goals were establishing techniques to decrease surgery times, reduce costs, and maintain compatibility with existing laboratory systems such as primate chairs and recording apparatuses. We addressed these issues by forming titanium footed headposts pre-operatively using 3D printed skull replicas of each animal, using free and open-source software wherever possible, and by adapting headpost procedures in three different laboratories and assembling an inexpensive system of clamps to mate the headpost with a primate chair at any angle. We describe timeline considerations, including time required for each step as well as healing time for headposts to osseointegrate properly. In our experience, the acrylic free implants are about three times more expensive than the acrylic implants ($1800 vs ~$600) when taking into account only the headposts themselves and the screws. However, the main advantages to acrylic free implants are the longevity of the implant, allowing the animals to be used for long duration, chronic experiments (>4 years in our experience) eliminating the need to do multiple implants, explants, and re-implants, and the dramatic reduction in surgery time for the surgeon (from 3-4 hours to an hour or less). Regarding outcomes, skin regression and bone exposure are a major concern for footed titanium headposts. It is difficult to directly compare the disadvantages of the skin regression with the titanium headposts to the relative lack of this issue with acrylic implants. However, while we found considerable variability with respect to skin regression and exposure of the metal implant, there was not a single case of bone exposure or other complication that would warrant removal of the implant. Nonetheless, these methods must be refined further in order to determine what implant properties and procedures could be implemented to improve skin-implant margin conditions. Ultimately, however, if acrylic-free methods are to be adopted, there must also be a streamlined method for designing and implanting an acrylic-free recording chamber along with the headpost. Our single case of a PEEK recording chamber failed due to recurrence of a previous infection so it is unknown what outcome could be expected in other cases using the same techniques. Overall, this is a important area of investigation that has the ability to significantly improve the welfare of research NHPs.

ACKNOWLEDGMENTS:

The authors thank Rhonda S. Oates, Angie M. Michaiel, Leah Krubitzer and Kenneth H. Britten for their contribution to this project. Special thanks to Saleda D. Moreland, Jamie R. Amaral, Hugo Vega-Ramirez and Adam D. Cook for exceptional animal care.

WORKS CITED

Adams DL, **Economides JR**, **Jocson CM**, **Horton JC**. A biocompatible titanium headpost for stabilizing behaving monkeys. *J Neurophysiol* 98: 993–1001, 2007.

Adams DL, **Economides JR**, **Jocson CM**, **Parker JM**, **Horton JC**. A watertight acrylic-free titanium recording chamber for electrophysiology in behaving monkeys. *J Neurophysiol* 106: 1581–1590, 2011.

Albrektsson T, **Brånemark PI**, **Hansson HA**, **Lindström J**. Osseointegrated titanium implants. Requirements for ensuring a long-lasting, direct bone-to-implant anchorage in man. *Acta Orthop Scand* 52: 155–170, 1981.

Amemori S, **Amemori K**, **Cantor ML**, **Graybiel AM**. A non-invasive head-holding device for chronic neural recordings in awake behaving monkeys. *J Neurosci Methods* 240: 154–160, 2015.

APIC. Guide to the Elimination of Orthopedic Surgical Site Infections [Online]. http://132889-www1.apic.org/Resource_/EliminationGuideForm/34e03612-d1e6-4214-a76b-e532c6fc3898/File/APIC-Ortho-Guide.pdf [15 Jan. 2017].

Aydin S, **Kucukyuruk B**, **Abuzayed B**, **Aydin S**, **Sanus GZ**. Cranioplasty: Review of materials and techniques. *J Neurosci Rural Pract* 2: 162–167, 2011.

Bergman H, **Deuschl G**. Pathophysiology of Parkinson's disease: From clinical neurology to basic neuroscience and back. *Mov Disord* 17: S28–S40, 2002.

Botha C. Extracting STL surface from CT data with DeVIDE [Online]. https://www.youtube.com/watch?v=_PtTpRz3aU8 [7 Oct. 2016].

Botha CP. Technical Report: DeVIDE—The Delft Visualisation and Image processing Development Environment. .

Burke SN, **Barnes CA**. Neural plasticity in the ageing brain. *Nat Rev Neurosci* 7: 30–40, 2006.

Buser D, **Schenk RK**, **Steinemann S**, **Fiorellini JP**, **Fox CH**, **Stich H**. Influence of surface characteristics on bone integration of titanium implants. A histomorphometric study in miniature pigs. *J Biomed Mater Res* 25: 889–902, 1991.

Caro-Osorio E, **De la Garza-Ramos R**, **Martínez-Sánchez SR**, **Olazarán-Salinas F**. Cranioplasty with polymethylmethacrylate prostheses fabricated by hand using original bone flaps: Technical note and surgical outcomes. *Surg Neurol Int* 4, 2013.

Chimutengwende-Gordon M, **Pendegrass C**, **Blunn G**. Enhancing the soft tissue seal around intraosseous transcutaneous amputation prostheses using silanized fibronectin titanium alloy. *Biomed Mater Bristol Engl* 6: 025008, 2011.

Davis RT, **Leathers CW**. *Behavior and pathology of aging in rhesus monkeys*. A.R. Liss, 1985.

Davis TS, **Torab K**, **House P**, **Greger B**. A minimally invasive approach to long-term head fixation in behaving nonhuman primates. *J Neurosci Methods* 181: 106–110, 2009.

Desimone R, **Duncan J**. Neural Mechanisms of Selective Visual-Attention. *Annu Rev Neurosci* 18: 193–222, 1995.

Donati L, **Quadri P**, **Reiner M**. Reactivation of Osteomyelitis Caused by Staphylococcus Aureus After 50 Years. *J Am Geriatr Soc* 47: 1035–1037, 1999.

Drucker CB, **Carlson ML**, **Toda K**, **DeWind NK**, **Platt ML**. Non-invasive primate head restraint using thermoplastic masks. *J Neurosci Methods* 253: 90–100, 2015.

Eley KA, **Watt-Smith SR**, **Golding SJ**. "Black bone" MRI: a potential alternative to CT when imaging the head and neck: report of eight clinical cases and review of the Oxford experience. *Br J Radiol* 85: 1457–1464, 2012.

Eley KA, **Watt-Smith SR**, **Golding SJ**. "Black Bone" MRI: a novel imaging technique for 3D printing. *Dento Maxillo Facial Radiol* 46: 20160407, 2017.

Eley KA, **Watt-Smith SR**, **Sheerin F**, **Golding SJ**. "Black Bone" MRI: a potential alternative to CT with three-dimensional reconstruction of the craniofacial skeleton in the diagnosis of craniosynostosis. *Eur Radiol* 24: 2417–2426, 2014.

Fan J, Li Y, Fu X, Li L, Hao X, Li S. Nonhuman primate models of focal cerebral ischemia. *Neural Regen Res* 12:321-328.

Fearnley JM, **Lees AJ**. Aging and Parkinson's disease: Substantia nigra regional selectivity. *Brain* 114: 2283–2301, 1991.

Genest AS. Cranioplasty made easier. *Surg Neurol* 10: 255–257, 1978.

Gergely RCR, Toohey KS, Jones ME, Small SR, Berend ME. towards the optimization of the preparation procedures of PMMA bone cement. *J. Orthopedic Res* 34:915-923, 2016.

Goodale MA, **Milner AD**. Separate visual pathways for perception and action. *Trends Neurosci* 15: 20–25, 1992.

Graziano MSA, **Taylor CSR**, **Moore T**, **Cooke DF**. The cortical control of movement revisited. *Neuron* 36: 349–362, 2002.

Hacking SA, **Boyraz P**, **Powers BM**, **Sen-Gupta E**, **Kucharski W**, **Brown CA**, **Cook EP**. Surface roughness enhances the osseointegration of titanium headposts in non-human primates. *J Neurosci Methods* 211: 237–244, 2012.

Holt BM, **Betz DH**, **Ford TA**, **Beck JP**, **Bloebaum RD**, **Jeyapalina S**. Pig dorsum model for examining impaired wound healing at the skin-implant interface of percutaneous devices. *J Mater Sci Mater Med* 24: 2181, 2013.

Hwang EJ, Hauschild M, Wilke M, Andersen RA. Inactivation of the parietal reach region causes optic ataxia, impairing reaches but not saccades. *Neuron* 76:1021-2029, 2012.

Isoda M, **Tsutsui K-I**, **Katsuyama N**, **Naganuma T**, **Saito N**, **Furusawa Y**, **Mushiake H**, **Taira M**, **Tanji J**. Design of a head fixation device for experiments in behaving monkeys. *J Neurosci Methods* 141: 277–282, 2005.

ISO/TC 261. ISO/ASTM 52900:2015 - Additive manufacturing -- General principles -- Terminology [Online]. 2015. http://www.iso.org/iso/catalogue_detail.htm?csnumber=69669 [22 Dec. 2016].

Johnston JM, Cohen YE, Shirley H, Tsunada J., Bennur S, Christison-Lagay K, Veeder CL. Recent refinements to cranial implants for rhesus macaques (*Macaca mulatta*) *Lab Anim(NY)* 45:180-186, 2016.

Khoury J, **Kirkpatrick SR**, **Maxwell M**, **Cherian RE**, **Kirkpatrick A**, **Svrluga RC**. Neutral atom beam technique enhances bioactivity of PEEK. *Nucl Instrum Methods Phys Res Sect B Beam Interact Mater At* 307: 630–634, 2013.

Konecky RO, Smith MA, Olson CR. Monkey prefrontal neurons during Sternberg task performance: full contents of working memory or most recent item? *J Neurophysiol* 117:2269-2281, 2016.

Lai P-L, Tai C-L, Chu I-M, Fu T-S, Chen L-H, Chen W-J. Hypothermic manipulation of bone cement can extend the handling time during vertebroplasty. *BMC Musculoskeletal Disorders* 13: 198. doi: 10.1186/1471-2474-13-198.

Lanz F, **Lanz X**, **Scherly A**, **Moret V**, **Gaillard A**, **Gruner P**, **Hoogewoud H-M**, **Belhaj-Saif A**, **Loquet G**, **Rouiller EM**. Refined methodology for implantation of a head fixation device and chronic recording chambers in non-human primates. *J Neurosci Methods* 219: 262–270, 2013.

Lee S-C, **Wu C-T**, **Lee S-T**, **Chen P-J**. Cranioplasty using polymethyl methacrylate prostheses. *J Clin Neurosci Off J Neurosurg Soc Australas* 16: 56–63, 2009.

Leggat PA, **Smith DR**, **Kedjarune U**. Surgical applications of methyl methacrylate: a review of toxicity. *Arch Environ Occup Health* 64: 207–212, 2009.

Logothetis NK, Merkle H, Augath M, Trinath T, Ugurbil K. Ultra high-resolution fMRI in monkeys with implanted RF coils *Neuron* 35:227-242, 2002.

Lopez A, Hoess A, Thersleff T, Ott M, Engqvist H, Persson. Low-modulus PMMA bone cement modivied with castor oil. *Bio-Medical Materials and Engineering* 21:5-6, 323-332, 2011

Luck SJ, **Chelazzi L**, **Hillyard SA**, **Desimone R**. Neural mechanisms of spatial selective attention in areas V1, V2, and V4 of macaque visual cortex. *J Neurophysiol* 77: 24–42, 1997.

Ma R, **Tang T**. Current Strategies to Improve the Bioactivity of PEEK. *Int J Mol Sci* 15: 5426–5445, 2014.

Mandracci P, **Mussano F**, **Rivolo P**, **Carossa S**. Surface Treatments and Functional Coatings for Biocompatibility Improvement and Bacterial Adhesion Reduction in Dental Implantology. *Coatings* 6: 7, 2016.

Mangram AJ, **Horan TC**, **Pearson ML**, **Silver LC**, **Jarvis WR**. Guideline for prevention of surgical site infection, 1999. *Infect Control Hosp Epidemiol* 20: 250-278; quiz 279-280, 1999.

McAndrew RM, **Lingo VanGilder JL**, **Naufel SN**, **Helms Tillery SI**. Individualized recording chambers for non-human primate neurophysiology. *J Neurosci Methods* 207: 86–90, 2012.

Miller EK, **Cohen JD**. An integrative theory of prefrontal cortex function. *Annu Rev Neurosci* 24: 167–202, 2001.

Mink JW. The basal ganglie: Focused selection and inhibition of competing motor programs. *Prog Neurobiol* 50: 381–425, 1996.

Miocinovic S, **Noecker AM**, **Maks CB**, **Butson CR**, **McIntyre CC**. Cicerone: stereotactic neurophysiological recording and deep brain stimulation electrode placement software system. In: *Operative Neuromodulation*, edited by Sakas DE, Simpson BA. Springer Vienna, p. 561–567.

Miocinovic S, **Zhang J**, **Xu W**, **Russo GS**, **Vitek JL**, **McIntyre CC**. Stereotactic neurosurgical planning, recording, and visualization for deep brain stimulation in non-human primates. *J Neurosci Methods* 162: 32–41, 2007b.

Morrison JH, **Baxter MG**. The ageing cortical synapse: hallmarks and implications for cognitive decline. *Nat Rev Neurosci* 13: 240–250, 2012.

Mulliken GH, **Bichot NP**, **Ghadooshahy A**, **Sharma J**, **Kornblith S**, **Philcock M**, **Desimone R**. Custom-fit radiolucent cranial implants for neurophysiological recording and stimulation. *J Neurosci Methods* 241: 146–154, 2015.

Nudo RJ, **Milliken GW**. Reorganization of movement representations in primary motor cortex following focal ischemic infarcts in adult squirrel monkeys. *J Neurophysiol* 75: 2144–2149, 1996.

Nudo RJ, **Wise BM**, **SiFuentes F**, **Milliken GW**. Neural substrates for the effects of rehabilitative training on motor recovery after ischemic infarct. *Science* 272: 1791–1794, 1996.

Panteli M, **Giannoudis PV**. Chronic osteomyelitis: what the surgeon needs to know. *EFORT Open Rev* 1: 128–135, 2016.

Parker AJ, **Newsome WT**. Sense and the single neuron: probing the physiology of perception. *Annu Rev Neurosci* 21: 227–277, 1998.

Pendegrass CJ, **Gordon D**, **Middleton CA**, **Sun SNM**, **Blunn GW**. Sealing the skin barrier around transcutaneous implants: in vitro study of keratinocyte proliferation and adhesion in response to surface modifications of titanium alloy. *J Bone Joint Surg Br* 90: 114–121, 2008.

Pendegrass CJ, **Lancashire HT**, **Fontaine C**, **Chan G**, **Hosseini P**, **Blunn GW**. Intraosseous transcutaneous amputation prostheses versus dental implants: a comparison between keratinocyte and gingival epithelial cell adhesion in vitro. *Eur Cell Mater* 29: 237–249, 2015.

Pfingst BE, **Albrektsson T**, **Tjellström A**, **Miller JM**, **Zappia J**, **Xue X**, **Weiser F**. Chronic skull-anchored percutaneous implants in non-human primates. *J Neurosci Methods* 29: 207–216, 1989.

Pitkin M. Design features of implants for direct skeletal attachment of limb prostheses. *J Biomed Mater Res A* 101: 3339–3348, 2013.

Plautz EJ, **Milliken GW**, **Nudo RJ**. Effects of repetitive motor training on movement representations in adult squirrel monkeys: Role of use versus learning. *Neurobiol Learn Mem* 74: 27–55, 2000.

Plecko M, **Sievert C**, **Andermatt D**, **Frigg R**, **Kronen P**, **Klein K**, **Stübinger S**, **Nuss K**, **Bürki A**, **Ferguson S**, **Stoeckle U**, **Rechenberg B von**. Osseointegration and biocompatibility of different metal implants - a comparative experimental investigation in sheep. *BMC Musculoskelet Disord* 13: 1–12, 2012.

Potts LF, Wu H, Singh A, Marcilla I, Luquin MR, Papa SM. Modeling Parkinson's disease in monkeys for translational studies, a critical analysis. *Exp Neurol* 256:133-143, 2014.

Sperka DJ, **Ditterich J**. Splash: A Software Tool for Stereotactic Planning of Recording Chamber Placement and Electrode Trajectories. *Front Neuroinformatics* 5, 2011.

Squire LR, **Zola-Morgan S**. The Medial Temporal Lobe Memory System. *Science* 253: 1380–1386, 1991.

Stevens QEJ, **Seibly JM**, **Chen YH**, **Dickerman RD**, **Noel J**, **Kattner KA**. Reactivation of dormant lumbar methicillin-resistant Staphylococcus aureus osteomyelitis after 12 years. *J Clin Neurosci* 14: 585–589, 2007.

Sunara A, DeAngelish GC, Angelaki DC. Joint representation of tranlationa and rotational components of optic flow in parietal cortex. *Proc Natl Acad Sci (USA)* 113:5077-5082, 2016.

Tai C-L, Lai P-L, Lin W-D, Tsai T-T, Lee Y-C, Liu M-Y, Chen L-H. Modification of mechanical properties, polymerization temperature, and handling time of polymethylmethacrylate cement for enhancing applicability in vertebroplasty.. *BioMed Research International* 2016, Article ID 7901562, 2016.

Tjellström A, **Lindstrom J**, **Hallen O**, **Albrektsson T**, **Brånemark PI**. Osseointegrated titanium implants in the temporal bone: a clinical study on bone-anchored hearing aids. *J Otol* 2: 304–310, 1981.

Trisi P, **Rao W**, **Rebaudi A**, **Fiore P**. Histologic effect of pure-phase beta-tricalcium phosphate on bone regeneration in human artificial jawbone defects. *Int J Periodontics Restorative Dent* 23: 69–78, 2003.

Uçkay I, **Assal M**, **Legout L**, **Rohner P**, **Stern R**, **Lew D**, **Hoffmeyer P**, **Bernard L**. Recurrent Osteomyelitis Caused by Infection with Different Bacterial Strains without Obvious Source of Reinfection. *J Clin Microbiol* 44: 1194–1196, 2006.

Urist MR, **Nilsson O**, **Rasmussen J**, **Hirota W**, **Lovell T**, **Schmalzreid T**, **Finerman GAM**. Bone Regeneration under the Influence of a Bone Morphogenetic Protein (BMP) Beta Tricalcium Phosphate (TCP) Composite in Skull Trephine Defects in Dogs. *Clin Orthop* 214: 295–304, 1987.

Verhoef BE, Maunsell JHR. Attention-related changes in correlated neuronal activity arise from normalization mechanisms. *Nat Neurosci* 20:969-977, 2017. **Wurtz RH**. Visual cortex neurons: response to stimuli during rapid eye movements. *Science* 162: 1148–1150, 1968.

Yun HC, **Branstetter JG**, **Murray CK**. Osteomyelitis in military personnel wounded in Iraq and Afghanistan. *J Trauma-Inj Infect Crit Care* 64: S163–S168, 2008.

FIGURE CAPTIONS

Figure 1. Diagram of the traditional polymethyl-methacrylate (PMMA, or "acrylic") implant (top) and acrylic-free titanium footed headpost (bottom). A) A parasagittal view of the acrylic implant shows how bone screws are used as anchors for the PMMA mass and the recording chamber and headpost are embedded in the PMMA. Cross-hatching on headpost and chamber represent knurling that allows the PMMA to "grab" the metal. The headpost is further stabilized with a cross-bar (shown in B), show as a circle in A. The anterior-posterior axis is shown in the inset. B) Drawing of a top-down view of a monkey head with an acrylic implant, showing the large size of the implant margin relative to the headpost and recording chamber. Screw positions are drawn to illustrate a typical configuration used to ensure a secure implant and shown in gray to indicate that they are beneath acrylic. C) A parasagittal view of a titanium footed headpost. Note that screws are flush with the top of the headpost feet, which are covered by skin. D) The skin/implant margin of the titanium footed headpost is limited to the circumference of the post itself. The implant feet are shaded light gray to illustrate that they are covered by skin.

Figure 2. Timeline of headpost implant procedures to accompany Table 1. This figure depicts the steps detailed in Table 1 according to two potential timelines in order to give the reader a sense of how much time to allocate for each step. The timeline on the left indicates a feasible timeline where all steps up to headpost surgery can be completed in 16 working days. The "Rush" timeline on the right shows a possible 7-day timeline. Note that printing times may vary by service and any procedure that requires coordination with other staff may incur delays.

Figure 3. Photographs of 3D printed skulls of case 1 (top) and case 4 (bottom). A) Skull printed on a ZPrinter model 450 after being cleaned and cured. B) Same skull as in A, shown mounted in a stereotax with sulci and perimeter of planned recording chamber marked with pencil. C) Skull printed on a Stratasys Objet Eden 260V shown still on printing tray with gel-like support material intact. Skull replica was cropped into two pieces using Netfabb in order to save cost of support material. D) Same skull as in C, after cleaning and before the two pieces were glued together using cyanoacrylate.

Figure 4. Gray Matter headpost formed on a 3D printed skull replica (case #2) shown from various angles. The aim is to maximum contact and minimize gaps between skull and implant. Small gaps are evident as shadows. For reference, the thickness of the headpost foot is 1.39 mm, screw holes are 3 mm in diameter at the base and 5 mm at the top of the countersink and the distance between screw holes is approximately 4.5 mm at base (~2.5 mm on top). A) Top front view. B) Oblique right frontal view. C) Front close-up view. D) Right side view, slightly oblique to show curvature of front feet over brow ridge and slight spacing at distal end of feet. E) Left side view. F) Top view, showing configuration of all feet

and screw holes on skull replica. Caudal right foot was cut to include only one screw to allow ample space for a recording chamber on right side of skull. The caudal left foot was intentionally left long as this was a large male animal and a large recording cylinder was later placed on the right side over the central sulcus and posterior parietal cortex.

Figure 5. Attaching headpost to primate chair using strut clamps. A) Frontal view of headpost attached to primate chair using a set of three Misumi strut clamps (two with a post and one without). Each clamp is labeled (1, 2, and 3) with a corresponding blown-out illustration for clarity. Axes of rotation are depicted for each component as a line with a curved arrow. The first strut clamp ("1") is attached to the headpost adaptor. The second strut clamp ("2") is attached to the post of clamp 1. The third strut clamp ("3") is attached to the post of clamp 2 and the chair adaptor which is attached to the primate chair arm and projects vertically. Clamp levers are used (black handles on clamps 1 and 2, and orange handles on clamp 3) to facilitate adjustments. B) Side view of the same configuration as in A. Clamp components are labeled as in A. Note the angle of the headpost relative to the vertical chair adaptor.

Figure 6. Design of customized recording chamber. A) Lateral view in Monkey Cicerone showing parasagittal MRI slice, position of recording chamber and a virtual electrode track, and an ear bar and eye bar (top). Verification of electrode tracks and planned recording sites in Monkey Cicerone in a coronal (bottom, left) and parasagittal view (bottom, right). B) Lateral view of skull STL in Meshmixer with recording chamber model positioned as planned. C) Inset shows four points that were selected in Meshmixer: three points to define the stereotaxic plane (two ear bar and one eye bar position, shown with orange stars) and one point to define the center of the cylinder on the skull surface (origin, marked with a red star). Cropped portion of skull model and three points defining the stereotaxic plane from Meshmixer (yellow, circled) shown after being imported into Inventor from Meshmixer (see inset). The user coordinate system (UCS) was defined using the origin (center of cylinder on skull surface) with the X axis oriented along the bore of the cylinder (in the direction of an electrode track).

Figure 7. 3D printed headpost covers. A) Original design that screwed onto headpost from the top. B) Improved "igloo" design that screwed from the front of the post. C) Side view of "igloo" showing profile designed to approximate the curvature of the head and brow ridge. Excess material was sanded off after printing to ensure hat did not touch skin.

Figure 8. Implant margin condition for all 9 cases. Conditions of the skin at the implant margin were categorized into four groups. Skin recession (diagonal bars) indicates the earliest signs of skin recession from the post, such as redness, moistness, or proliferation of granulation tissue. Metal exposure (dark gray) indicates from 1 to 4 mm exposure of one or more titanium feet. Screw exposure (gray cross-hatch)

resulted when skin recession was greater than 4 mm along a foot. Note absence of bone exposure in all cases regardless of degree or duration of skin recession. Asterisks (*) indicate deceased cases (see Table 1).

TABLES

TABLE 1. OVERVIEW OF HEADPOST PROCEDURES

Step #	Procedure	Time to complete step	Materials & Resources	Notes
1	**CT scan of head**	~2 hours	CT scanner, Vet personnel	Perform CT (slices ≤ 0.6 mm) within 6 months of new implant; bone can remodel quickly, especially after a previous implant is removed
2	**Create STL model from CT data**	< 1 hours	DeVIDE or InVesalius	Extract bone surface contour from CT data to produce a 3D printable model (an STL file).
3	**Crop and repair STL model**	1-3 hours	NetFabb Basic and/or Meshmixer	Use 3D modeling software with "STL repair" capability to crop and repair STL file as desired. Optional: cut digital skull model into two pieces to cut cost of support material used during printing. Use NetFabb to check printability of part(s)
4	**Print skull replica**	Varies (~1-3 days)	3D printer or printing service	Check with printer in advance for turnaround time estimates. Recommended minimum 300 dpi resolution: 300 dpi (85 μm feature size).
5	**Determine location of headpost on skull**	2-3 days (do while skull is being printed)	Monkey Cicerone or SPLASH (requires structural MRI)	Identify target brain areas and potential locations of recording cylinders or other implant hardware that will constrain headpost location. This can also be done using gyrus patterns on interior surface of printed skull model.
6	**Bend headpost feet to fit skull**	6-8 hours	Gray Matter headpost & bending bars, skull replica	Use 3D skull replica to form footed headpost before surgery. Bend slowly, making small incremental adjustments and working proximal to distal. Target 1-mm maximum gap between bone and titanium.
7	**Estimate screw lengths**	< 30 min	RadiANT DICOM viewer	Measure skull thickness in DCM viewer, or drill holes in skull model and measure with depth gauge to estimate appropriate screw lengths. Screws threads must reach through both inner and outer cortical tables of bone. Pack 1-2 extra sets of each length of screw.
8	**Headpost implant surgery**	~2 hours	Follow Gray Matter surgery guidelines for U-shaped incision. Drill holes quickly and smoothly with burr size slightly smaller than core diameter of screw. Use Fusion Bone Putty to fill gaps between bone and implant. Screws must seat fully into implant countersinks, but do not overtighten.	
9	**Allow healing time**	Allow a minimum of 4-5 weeks, up to 12 weeks	Use this time to acclimate animal to lab settings, personnel and head restraint procedures. For example, begin by presenting headpost coupler and hovering over head, then gradually touching post, inserting coupler slot onto post and removing without attaching the coupler with a screw. This process can take several weeks with a new monkey and will save time once healed.	
10	**Attach headpost to chair**	Headpost training varies (~1-2 days once acclimated)	Misumi post & strut clamps	Clamp angles can be modified to adjust head position and maximize animal's comfort in the chair. Each animal/chair combination can have it's own set of clamps that will rarely need adjusting once done properly.

TABLE 2. SUBJECT INFORMATION AND TIMELINE

Case #	Sex	Weight (kg)	Age at implant (yrs)	CT prior to surgery (days)	STL prior to surgery (days)	3D print prior to surgery (days)
1	F	9.0	6.9	139	138	120
2	M	13.0	5.6	14	14	13
3	M	13.5	12.9	173	172	154
4	M	9.0	29.3	155	52	35
5	F	6.0	10.6	28	27	25
6	M	13.0	12.9	140	29	23
7	F	9.0	12.0	15	10	not recorded
8	F	8.0	9.1	62	not recorded	not recorded
9	F	9.0	7.6	154	not recorded	not recorded

Subject information and experimental timeline. Cases are numbered in chronological order of procedure. Ages reported are at the time of headpost implant. Timeline information is relative to date of headpost implant for each case: CT scan in days prior to surgery; conversion of CT data to digital model (STL format) and 3D printing of skull replica, also in days prior to surgery.

TABLE 3.1. SOFTWARE

Software	URL (or contact)	Cost
DeVIDE	https://graphics.tudelft.nl/devide/	Free
InVesalius	http://www.cti.gov.br/invesalius/	Free
NetFabb Basic	http://www.autodesk.com/education/free-software/netfabb	Free
Meshmixer	http://www.meshmixer.com/	Free
Monkey Cicerone	(contact author CCM)	Free
SPLASh (Linux)	http://systems.ucdavis.edu/splash/splash.html	Free
Inventor	http://www.autodesk.com/education/free-software/inventor-professional	Varies (Institutional license available)

TABLE 3.2. PARTS, SUPPLIERS AND PRICES

Product	Supplier and URL	Part Number	Cost	Qty	Total
Titanium footed headpost	Gray Matter http://www.graymatter-research.com/	Complete system (DAHP-1)	$1600	1	$1600
Bone screws ($20 ea.)		BS-1 (specify size)	(22 included with DAHP)		
Fusion Bone Putty (1 cc)	Veterinary Transplant Services https://vtsonline.com/	FXBP1cc	$68	1	$68

Clamp Levers - Threaded	MISUMI https://us.misumi-ec.com/	CLMS4-16-R	$15.15	2	$30
Strut Clamps - Arm Type, P Selectable		ALKA12-50	$22.22	2	$44
Strut Clamps - With Clamp Lever, Perpendicular Configuration		AKST12	$39.60	1	$40
				TOTAL:	$1,782

TABLE 4. FACTORS THAT MAY INFLUENCE HEADPOST OR IMPLANT MARGIN OUTCOME

Case #	**Lab/ surgeon**	**Previous acrylic implant?**	**Headpost**	**Incision**	**# of screws**	**Healing time (weeks)**	**Years with headpost**	**Metal or screw exposure?**
1	1	No	custom type 1 (machined fit)	midline	10	4	*0.7*(de)*	Yes
2	1	No	DAHP-2 (Gray Matter)	midline	13	6	*4.0*(de)*	No
3	2	Yes	DAHP-2 (Gray Matter)	U-shaped	11	12 or more	4.5+	Yes
4	2	Yes	DAHP-2 (Gray Matter)	U-shaped	12	12 or more	*1.6*(dn)*	No
5	3	No	custom type 2 (manually bent)	U-shaped	11	5	3.8+	Yes
6	2	Yes	DAHP-2 (Gray Matter)	U-shaped	12	4	3.6+	Yes
7	1	No	DAHP-2 (Gray Matter)	U-shaped	14	not recorded	*1.6*(de)*	Yes
8	3	No	custom type 2 (manually bent)	midline	11	not recorded	3.4+	Yes
9	3	No	custom type 2 (manually bent)	midline	11	not recorded	2.9+	Yes

Factors that may influence headpost or implant margin outcomes. As in Table 2 (Subject Information), cases are numbered in chronological order of procedure. Refer to Table 2 for subject sex, age, and weight. Three animals had previously had an acrylic implant (cases 3, 4 and 6). Healing time between implant surgery and first attempted head restraint is reported in weeks following surgery. Total duration with headpost implanted is given in years. Cases indicated with an asterisk (*), 1, 4 and 7, are deceased of natural causes (dn) or experimental design (de). Remaining cases are currently still enrolled in studies (as of August 2017) and headposts are intact and used regularly.

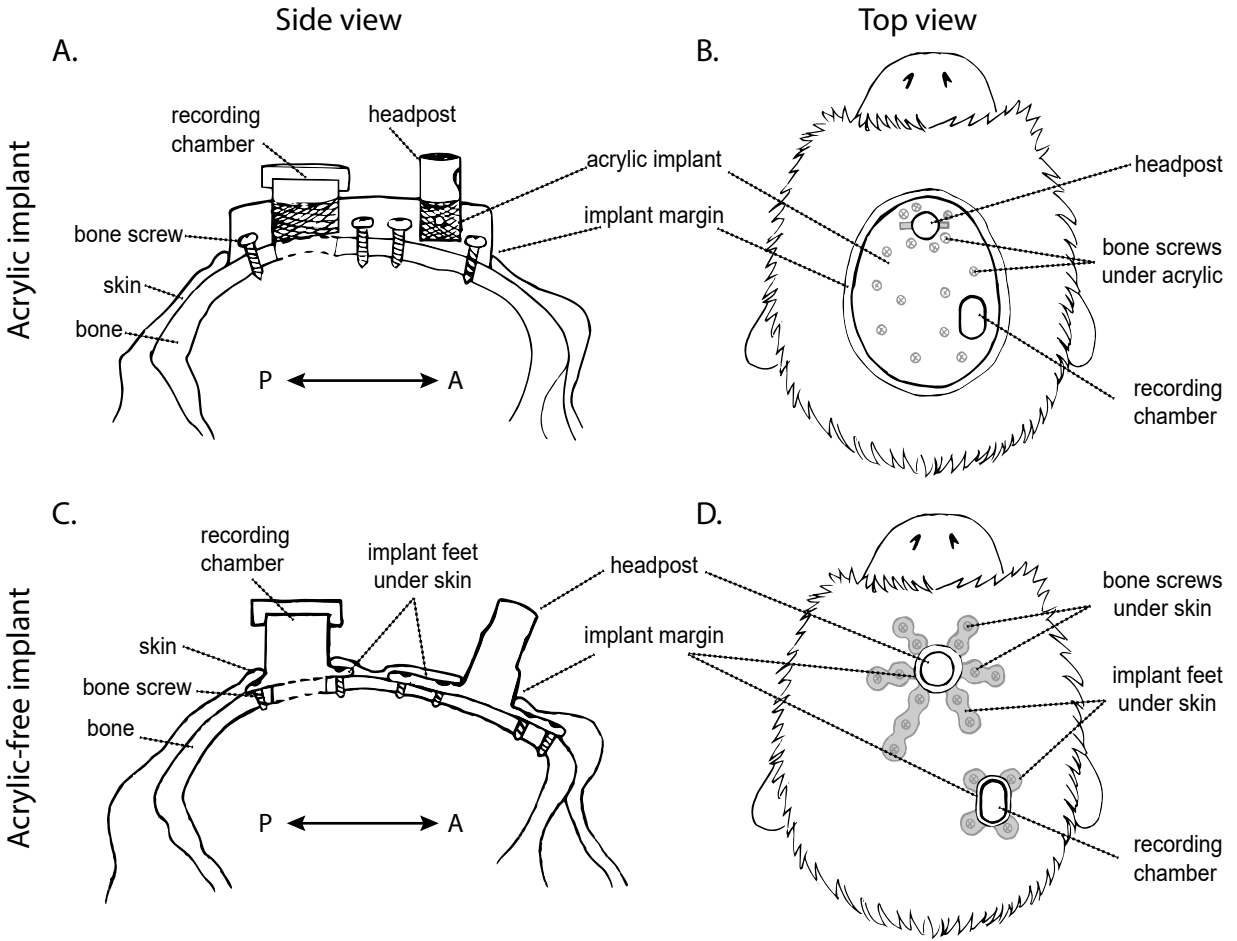
Side view
Top view
A.
B.
Acrylic implant
recording chamber
headpost
acrylic implant
implant margin
bone screw
skin
bone
P
A
headpost
bone screws under acrylic
recording chamber
C.
D.
Acrylic-free implant
recording chamber
implant feet under skin
headpost
implant margin
skin
bone screw
bone
P
A
bone screws under skin
implant feet under skin
recording chamber

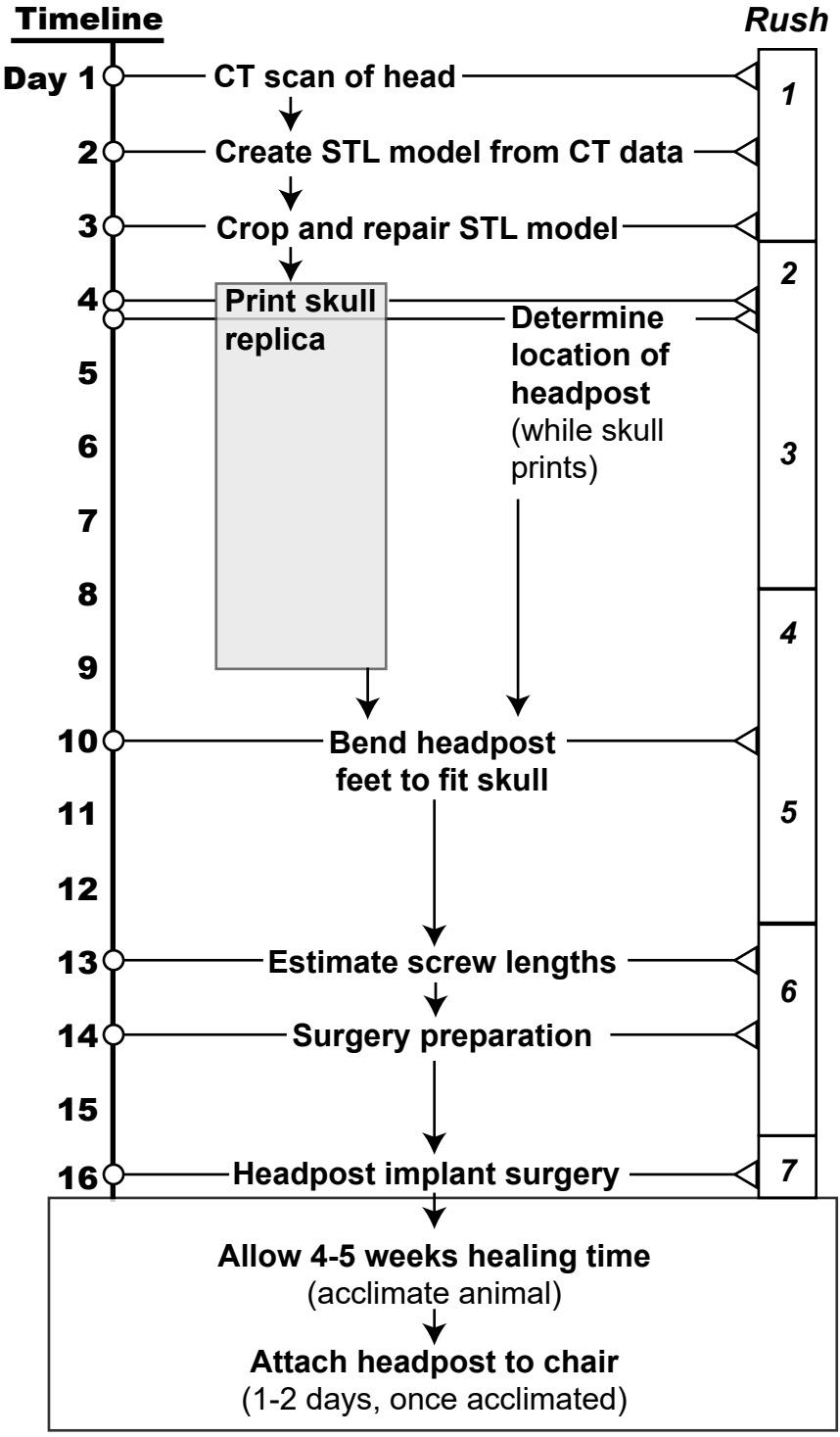
Timeline
Rush
Day 1
CT scan of head
2
Create STL model from CT data
3
Crop and repair STL model
4
Print skull replica
Determine location of headpost (while skull prints)
5
6
7
8
9
10
Bend headpost feet to fit skull
11
12
13
Estimate screw lengths
14
Surgery preparation
15
16
Headpost implant surgery
1
2
3
4
5
6
7
Allow 4-5 weeks healing time
(acclimate animal)
Attach headpost to chair
(1-2 days, once acclimated)

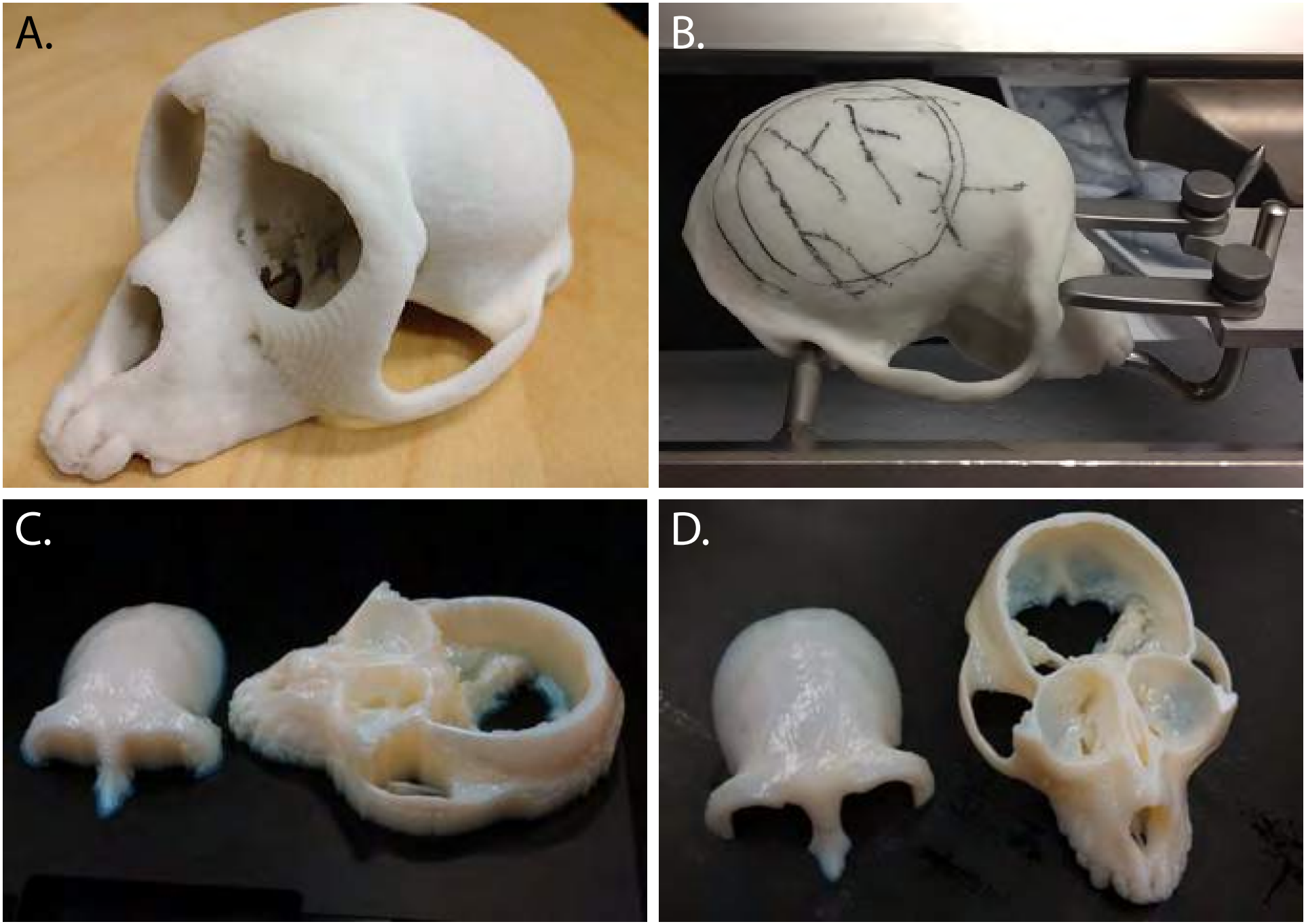
A.
B.
C.
D.

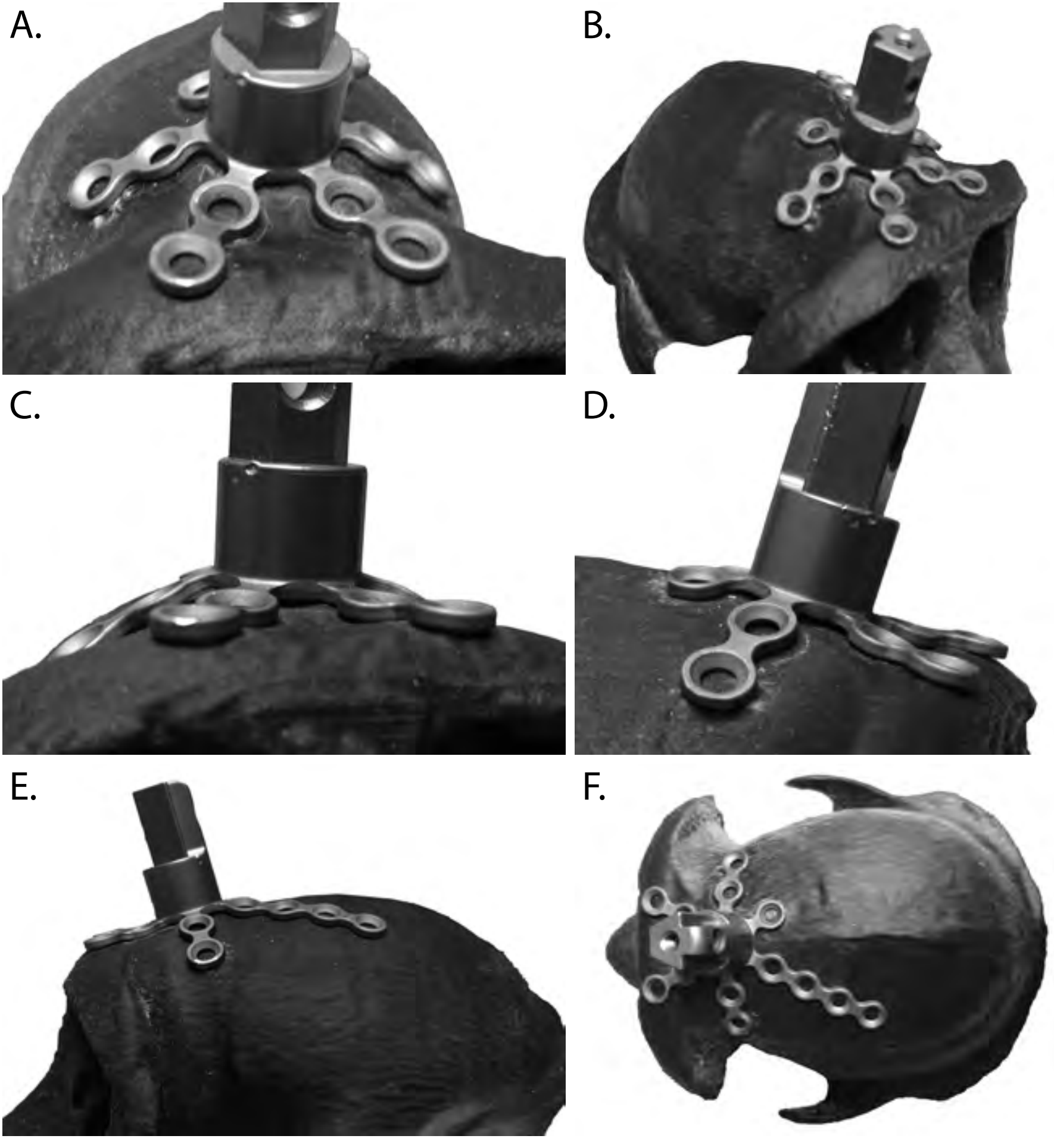
A.
B.
C.
D.
E.
F.

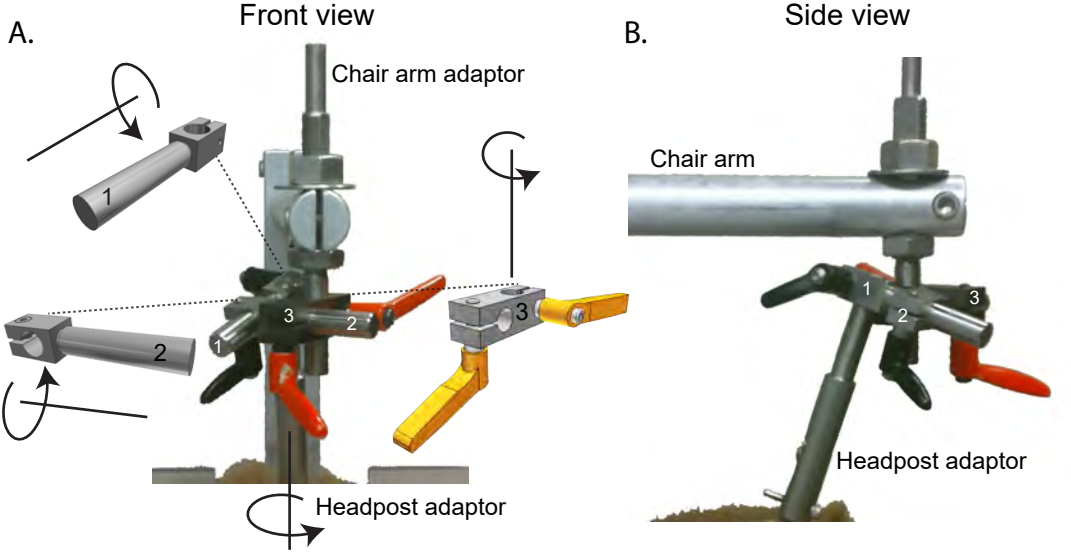
A.
Front view
Chair arm adaptor
1
2
3
1
2
3
Headpost adaptor
B.
Side view
Chair arm
1
2
3
Headpost adaptor

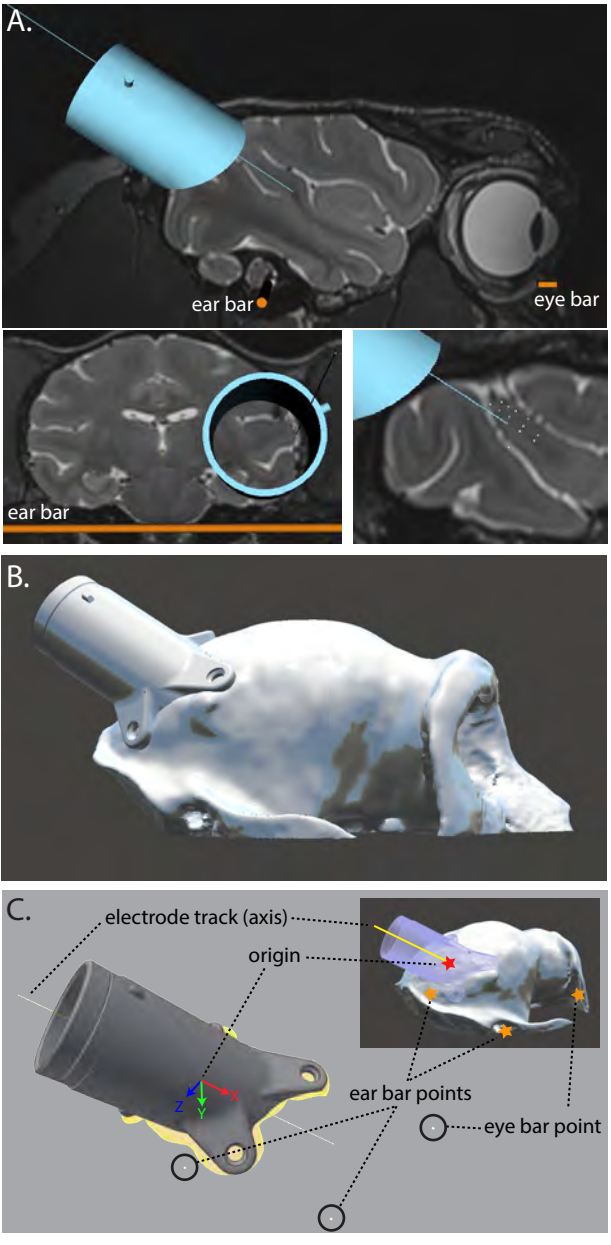
A.
ear bar
eye bar
ear bar
B.
C.
electrode track (axis)
origin
ear bar points
eye bar point

A.

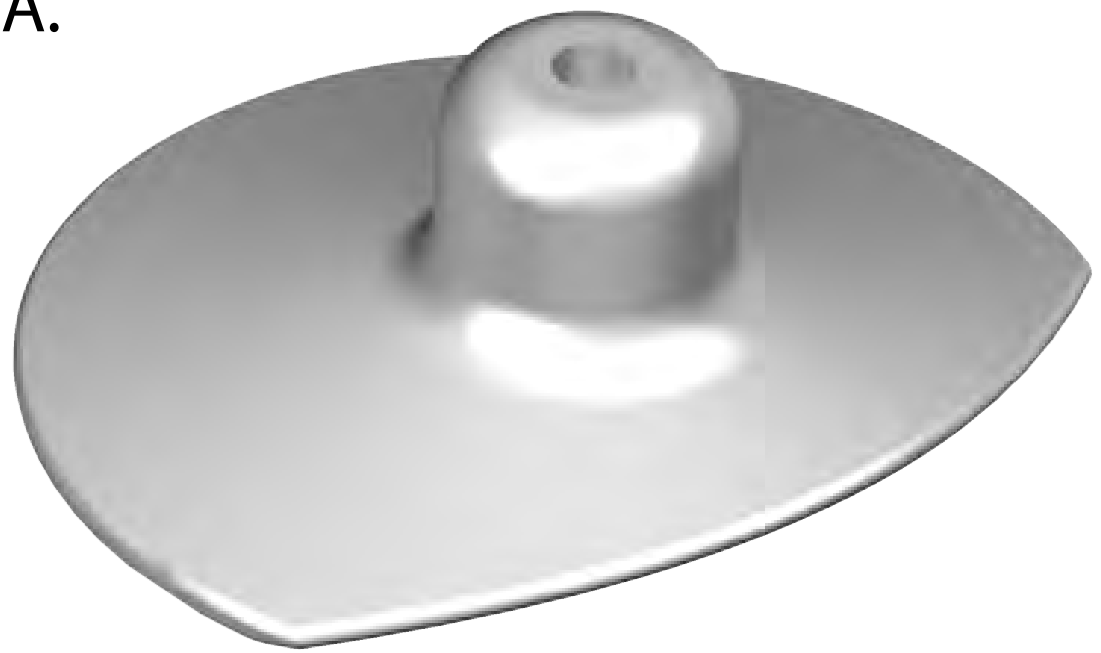

B.

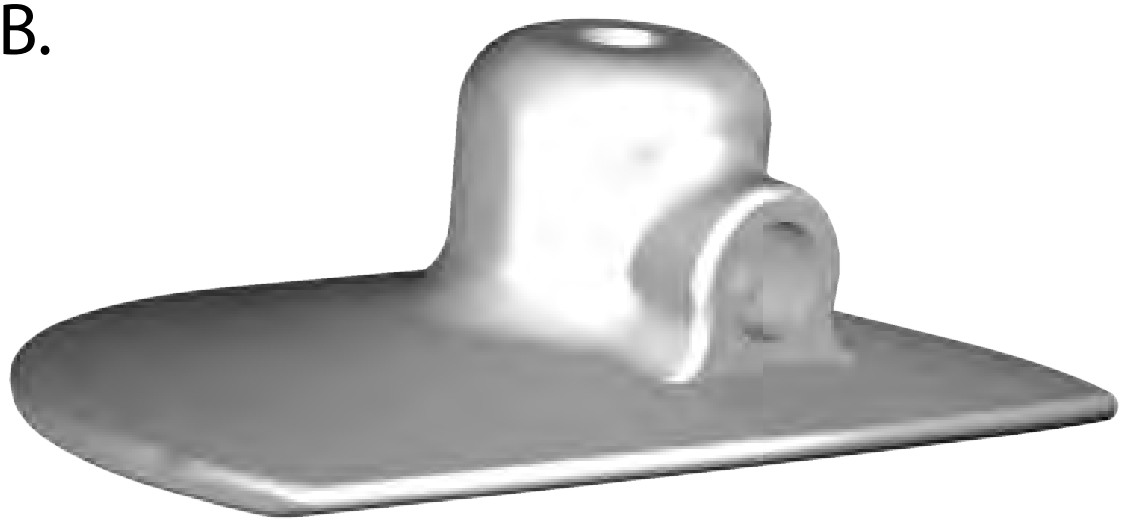

C.

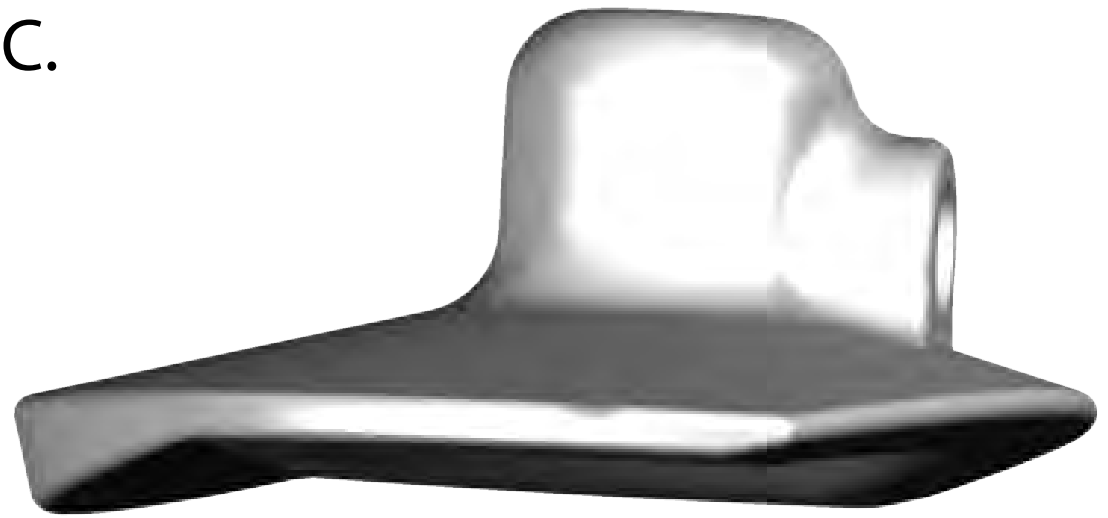

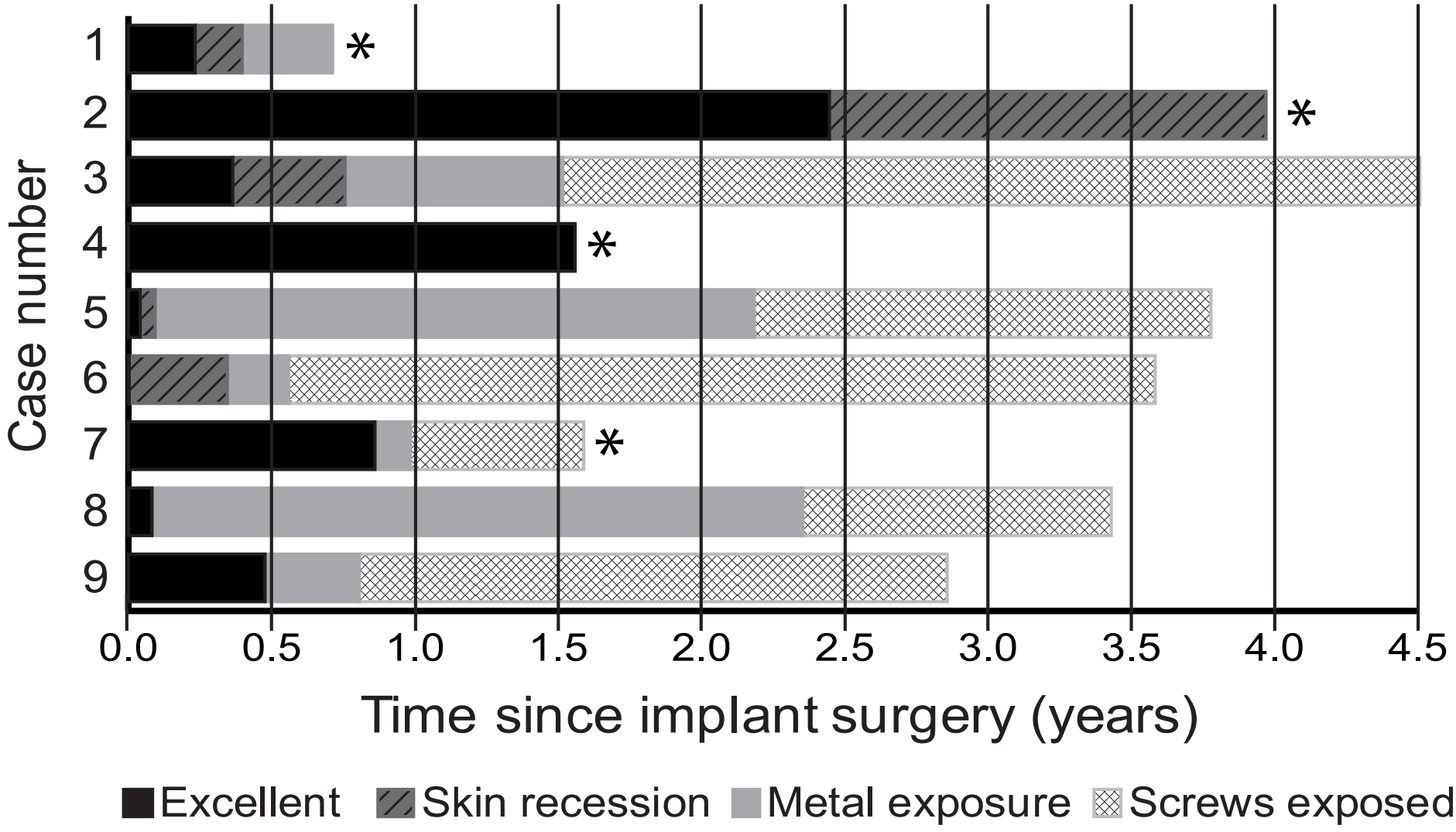
Case number
1
2
3
4
5
6
7
8
9
*
*
*
0.0
0.5
1.0
1.5
2.0
2.5
3.0
3.5
4.0
4.5
Time since implant surgery (years)
Excellent
Skin recession
Metal exposure
Screws exposed